

# AgriRisk Climate and climate projection data: methods and overview of results

---

Timothy Lynam

Reflecting Society

March 15<sup>th</sup>, 2018



***Risk Proofing Nova Scotia Agriculture: A Risk Assessment System Pilot (AgriRisk)***

*Nova Scotia Federation of Agriculture would like to recognize the collaborative relationships that exist among Agriculture and Agri-Food Canada and the Nova Scotia Departments of Agriculture and Environment.*

*Copyright 2018 ©. No license is granted in this publication and all intellectual property rights, including copyright, are expressly reserved. This publication shall not be copied except for personal, non-commercial use. Any copy must clearly display this copyright.*

*While the information in this publication is believed to be reliable when created, accuracy and completeness cannot be guaranteed. Use the publication at your own risk. Any representation, warranty, guarantee or conditions of any kind, whether express or implied with respect to the publication is hereby disclaimed. The authors and publishers of this report are not responsible in any manner for any direct, indirect, special or consequential damages or any other damages of any kind howsoever caused arising from the use of this Report.*

## Acknowledgements

I am indebted and most grateful for the many contributions made, by individuals and organisations, to developing these data sets. In particular, Dan McKenney, Pia Papadopol, Kevin Lawrence and David Price of NRCan were extraordinarily generous with data and guidance.

Through their funding and in-kind contributions AAFC, NSDA, NSE and NSFA made this work possible. Thank you.

Meredith Flannery, Jen Graham and Mark MacPherson provided support and a wonderfully solid management team to work with. Thank you.

The R community, without whom, none of this would have been possible, thank you.

## Table of Contents

Acknowledgements.....	iii
List of Figures .....	iv
List of tables .....	vii
Introduction .....	- 1 -
Methodological overview .....	- 1 -
Climate station data .....	- 1 -
Baseline climate surfaces .....	- 2 -
Daily climate projections .....	- 2 -
Overview of the projection data .....	- 7 -
Distributional assumptions .....	- 7 -
Growing degree days (GDD).....	- 7 -
Counts of days exceeding thresholds .....	- 8 -
Mapping of key variables and change relative to baseline.....	- 12 -
Growing degree days .....	- 13 -
Frost free days (FFD) .....	- 19 -
Days with minimum temperature less than -19°C.....	- 22 -
Days with minimum temperature less than -23°C.....	- 26 -
Summary .....	- 30 -
References cited .....	- 32 -
Appendix 1: Climate station data – stations names, ID’s and time periods of data downloaded....	- 33 -

## List of Figures

Figure 1. Map of sample points used for examination of distributional assumptions. ....	- 4 -
Figure 2. GDD estimates for base 10, April to October 2030 to 2040 (i.e. centred on 2035) for Bridgewater, fit to gamma distribution. ....	- 7 -
Figure 3. GDD estimates for base 10, April to October 2030 to 2040 (i.e. centred on 2035) for Halifax International Airport, fit to gamma distribution. ....	- 8 -
Figure 4. Count of FFD (using base 0) per year for the period 2020 to 2030 (i.e. centred on 2025) for Liverpool Milton, fit to Gamma distribution. ....	- 9 -
Figure 5. Count of FFD (using base 0) per year for the period 2030 to 2040 (i.e. centred on 2035) for Liverpool Milton, fit to gamma distribution. ....	- 9 -
Figure 6. Count of FFD (using base 0) per year for the period 2020 to 2030 (i.e. centred on 2025) for Halifax International Airport, fit to gamma distribution.....	- 10 -
Figure 7. Count of FFD (using base 0) per year for the period 2030 to 2040 (i.e. centred on 2035) for Halifax International Airport, fit to gamma distribution.....	- 10 -

Figure 8. Count of days less than -23°C per year for the period 2020 to 2030 (i.e. centred on 2025) for Bridgewater, fit to negative binomial distribution. ....	11 -
Figure 9. Count of days less than -23°C per year for the period 2030 to 2040 (i.e. centred on 2035) for Bridgewater, fit to negative binomial distribution. ....	11 -
Figure 10. Count of days less than -18°C per year for the period 2030 to 2040 (i.e. centred on 2035) for Collegeville, fit to negative binomial distribution. ....	12 -
Figure 11. Count of days less than -18°C per year for the period 2030 to 2040 (i.e. centred on 2035) for Halifax International Airport, fit to negative binomial distribution. ....	12 -
Figure 12. GDD 1970 to 2013. Top left: simulated mean GDD; top right, lower limit of the 95% CI for the mean; centre left, upper limit to the 95% CI; centre right NRCan modelled mean; bottom left, NRCan mean minus simulated mean; bottom right, NRCan mean / simulated mean. ....	13 -
Figure 13. Maps of changes in GDD (relative to 1970 to 2013 baseline) for 2020 projection period. Top left: simulated mean GDD; top right, lower limit of the 95% CI for the mean; centre left, upper limit to the 95% CI; centre right baseline (modelled) mean for 1970 to 2013; bottom left, baseline mean minus simulated mean; bottom right, baseline mean / simulated mean. ....	14 -
Figure 14. Maps of changes in GDD (relative to 1970 to 2013 baseline) for 2025 projection period. Top left: simulated mean GDD; top right, lower limit of the 95% CI for the mean; centre left, upper limit to the 95% CI; centre right baseline (modelled) mean for 1970 to 2013; bottom left, baseline mean minus simulated mean; bottom right, baseline mean / simulated mean. ....	15 -
Figure 15. Maps of changes in GDD (relative to 1970 to 2013 baseline) for 2030 projection period. Top left: simulated mean GDD; top right, lower limit of the 95% CI for the mean; centre left, upper limit to the 95% CI; centre right baseline (modelled) mean for 1970 to 2013; bottom left, baseline mean minus simulated mean; bottom right, baseline mean / simulated mean. ....	16 -
Figure 16. Maps of changes in GDD (relative to 1970 to 2013 baseline) for 2035 projection period. Top left: simulated mean GDD; top right, lower limit of the 95% CI for the mean; centre left, upper limit to the 95% CI; centre right baseline (modelled) mean for 1970 to 2013; bottom left, baseline mean minus simulated mean; bottom right, baseline mean / simulated mean. ....	17 -
Figure 17. Maps of changes in GDD (relative to 1970 to 2013 baseline) for 2050 projection period. Top left: simulated mean GDD; top right, lower limit of the 95% CI for the mean; centre left, upper limit to the 95% CI; centre right baseline (modelled) mean for 1970 to 2013; bottom left, baseline mean minus simulated mean; bottom right, baseline mean / simulated mean. ....	18 -
Figure 18. Maps of 95% CI widths (upper – lower) for each projection period with the width as a proportion of the mean for 2050 at bottom right. ....	19 -
Figure 19. Maps of changes in frost free days (FFD) relative to 1970 to 2013 baseline for 2025 projection period. Top left: simulated mean FFD; top right, lower limit of the 95% CI for the mean; centre left, upper limit to the 95% CI; centre right baseline (modelled) mean FFD for 1970 to 2013; bottom left, baseline mean minus simulated mean; bottom right, baseline mean / simulated mean. .-	20 -
Figure 20. Maps of changes in frost free days (FFD) relative to 1970 to 2013 baseline for the 2035 projection period. Top left: simulated mean FFD; top right, lower limit of the 95% CI for the mean; centre left, upper limit to the 95% CI; centre right baseline (modelled) mean FFD for 1970 to 2013; bottom left, baseline mean minus simulated mean; bottom right, baseline mean / simulated mean. .-	21 -
Figure 21. Maps of changes in frost free days (FFD) relative to 1970 to 2013 baseline for the 2050 projection period. Top left: simulated mean FFD; top right, lower limit of the 95% CI for the mean;	

centre left, upper limit to the 95% CI; centre right baseline (modelled) mean FFD for 1970 to 2013; bottom left, baseline mean minus simulated mean; bottom right, baseline mean / simulated mean. . - 22 -

Figure 22. Comparison of simulated versus NRCan modelled days with a minimum temperature less than -19°C (DL19) for the 1970 to 2013 period. Top left: simulated mean DL19; top right, lower limit of the 95% CI for the mean; centre left, upper limit to the 95% CI; centre right NRCan (modelled) mean DL19 for 1970 to 2013; bottom left, baseline mean minus simulated mean; bottom right, baseline mean / simulated mean..... - 23 -

Figure 23. Maps of changes in the number of days less than -19°C (DL19) relative to the simulated 1970 to 2013 baseline for the 2025 projection period. Top left: simulated mean DL19; top right, lower limit of the 95% CI for the mean; centre left, upper limit to the 95% CI; centre right baseline (modelled) mean DL19 for 1970 to 2013; bottom left, baseline mean minus simulated mean; bottom right, baseline mean / simulated mean. .... - 24 -

Figure 24. Maps of changes in the number of days less than -19°C (DL19) relative to the simulated 1970 to 2013 baseline for the 2035 projection period. Top left: simulated mean DL19; top right, lower limit of the 95% CI for the mean; centre left, upper limit to the 95% CI; centre right baseline (modelled) mean DL19 for 1970 to 2013; bottom left, baseline mean minus simulated mean; bottom right, baseline mean / simulated mean. .... - 25 -

Figure 25. Maps of changes in the number of days less than -19°C (DL19) relative to the simulated 1970 to 2013 baseline for the 2050 projection period. Top left: simulated mean DL19; top right, lower limit of the 95% CI for the mean; centre left, upper limit to the 95% CI; centre right baseline (modelled) mean DL19 for 1970 to 2013; bottom left, baseline mean minus simulated mean; bottom right, baseline mean / simulated mean. .... - 26 -

Figure 26. Comparison of simulated versus NRCan modelled days with a minimum temperature less than -23°C (DL23) for the 1970 to 2013 period. Top left: simulated mean DL23; top right, lower limit of the 95% CI for the mean; centre left, upper limit to the 95% CI; centre right NRCan (modelled) mean DL23 for 1970 to 2013; bottom left, baseline mean minus simulated mean; bottom right, baseline mean / simulated mean..... - 27 -

Figure 27. Maps of changes in the number of days less than -23°C (DL23) relative to the simulated 1970 to 2013 baseline for the 2025 projection period. Top left: simulated mean DL23; top right, lower limit of the 95% CI for the mean; centre left, upper limit to the 95% CI; centre right baseline (modelled) mean DL23 for 1970 to 2013; bottom left, baseline mean minus simulated mean; bottom right, baseline mean / simulated mean. .... - 28 -

Figure 28. Maps of changes in the number of days less than -23°C (DL23) relative to the simulated 1970 to 2013 baseline for the 2035 projection period. Top left: simulated mean DL23; top right, lower limit of the 95% CI for the mean; centre left, upper limit to the 95% CI; centre right baseline (modelled) mean DL23 for 1970 to 2013; bottom left, baseline mean minus simulated mean; bottom right, baseline mean / simulated mean. .... - 29 -

Figure 29. Maps of changes in the number of days less than -23°C (DL23) relative to the simulated 1970 to 2013 baseline for the 2050 projection period. Top left: simulated mean DL23; top right, lower limit of the 95% CI for the mean; centre left, upper limit to the 95% CI; centre right baseline (modelled) mean DL23 for 1970 to 2013; bottom left, baseline mean minus simulated mean; bottom right, baseline mean / simulated mean. .... - 30 -

**List of tables**

Table 1. Ensemble of GCM model simulations used in the projection analysis. ....- 2 -

## Introduction

Reflecting Society was contracted by the Nova Scotia Federation of Agriculture (NSFA) to provide climate and climate projection data for the AgriRisk project.

The climate data comprised: a) data from select climate stations in Nova Scotia; and b) daily climate projections for four periods (2020, 2025, 2030 and 2035). In both cases the following variables were requested (where available):

- minimum temperature (deg C)
- maximum temperature (deg C)
- precipitation (mm)
- relative humidity (%)
- snow depth (mm or m)

Baseline data for daily relative humidity and snow depth has not been provided. For relative humidity the disease modelling required hourly estimates of RH which was not available. Baseline snow depth was also not available.

In addition to these contractual requests the AgriRisk project required derived variables for use in the grape suitability and grape modelling parts of the project. The following variables were required:

- Growing degree days (GDD)
- Frost free days (FFD)
- The number of days with the daily minimum temperature less than -23, -19 and -18°C.

In this document the methods used to procure or generate these data sets are described.

The data are to be developed for five purposes:

- 1) As inputs to the grape suitability mapping;
- 2) As inputs to the GIS data viewer;
- 3) As inputs to the grape and wine modelling;
- 4) As inputs to the disease modelling;
- 5) Providing robust climate projection data for other users.

## Methodological overview

### Climate station data

All available daily data for all climate stations in Nova Scotia that had at least five years of data (as of late October 2017) were downloaded from the Government of Canada,



Department of Environment, Historical climate data services<sup>1</sup> and placed on the NSFA sftp site as .csv files. Altogether data for 220 climate stations was uploaded. A listing of the stations and period for which data were available for each station is available in Appendix 1.

All available hourly data was downloaded from each of the nine stations for which hourly data was available (Brier Island, Copper Lake, Greenwood A, Halifax Stanfield International Airport, Malay Falls, Shearwater A, Sydney A, Western Head and Yarmouth A).

Baseline climate surfaces

Baseline daily climate data for minimum and maximum temperature as well as precipitation were provided to AgriRisk by NRCan on approximately a 10km grid<sup>2</sup>. The methods used to derive these data are described in Pedlar et al. (2015). Grids for each day of each year 1970 to 2013 were used to derive estimates of the derived variables described above (i.e. GDD, FFD, days less than or greater than a threshold) as a baseline. The methods used for developing these estimates were the same as those described below for the climate projections. In addition to these derived variables maps of daily min and max temperatures and precipitation were provided to the AgriRisk project.

The NRCan baseline data were maps generated by statistical models developed using weather station data for the whole of Canada (McKenney, Pedlar, Papadopol, & Hutchinson, 2006).

Daily climate projections

Statistically downscaled climate scenarios were downloaded from the Pacific Climate Impacts Consortium (PCIC) data download portal<sup>3</sup> (Pacific Climate Impacts Consortium, 2014) for the two climate projection scenarios of interest (rcp45 and rcp85). A total of 36 simulations were downloaded for each projection period: 18 for each emissions scenario (rcp45 and rcp85) with 18 GCM simulations downscaled using each of two methods. The two methods (Bias-Correction Spatial Disaggregation (BCSD) and Bias Correction/Constructed Analogues with Quantile mapping reordering (BCCAQ)) are well documented and widely used (Bürger, Murdock, Werner, Sobie, & Cannon, 2012; Bürger, Sobie, Cannon, Werner, & Murdock, 2013; Werner & Cannon, 2015; Wood, Leung, Sridhar, & Lettenmaier, 2004).

Table 1. Ensemble of GCM model simulations used in the projection analysis.

GCM Ensemble used for projection
MPI-ESM-LR-r3
inmcm4-r1
CNRM-CM5-r1
CanESM2-r1
MRI-CGCM3-r1

<sup>1</sup> <http://climate.weather.gc.ca/>

<sup>2</sup> For the latitude / longitude of Nova Scotia this translated into about a 6.5 by 6.5 km grid.

<sup>3</sup> <https://pacificclimate.org/data/statistically-downscaled-climate-scenarios>

CCSM4-r2
MIROC5-r3
ACCESS1-0-r1
GFDL-ESM2G-r1

Data were downloaded for minimum daily temperature (tasmin), maximum daily temperature (tasmax) and precipitation (precip or pr)<sup>4</sup>. Each of the available data sets comprised the output (tasmin, tasmax, precip) of daily GCM simulations for the period 1950 to 2100 and for a climate scenario (rcp26, rcp45 and rcp85 were available). Data were downloaded from the selected GCM simulations for an 11-year period centred on each of five future time periods (2020, 2025, 2030, 2035 and 2050). For example, to produce the projections for 2020 data for the simulated period of 2015 to 2025 was used; to produce the 2025 projections data for the simulated period of 2020 to 2030 was used. Data were downloaded for a region 1.1 times the extent of a bounding box that enclosed the coastline boundary of Nova Scotia. All projection series for the five projection periods were provided to users as individual simulations for each variable for each year of the projection period clipped to the bounding box (see Figure 1).

Derived values (e.g. GDD, FFD, days exceeding each threshold) were estimated using all rcp45 and all rcp85 simulations available for a projection period. For GDD estimates matched simulations were used such that the tasmin and tasmax simulations used for each calculation were from the same GCM and downscaling method. The same set of tasmin simulation data were used for estimating FFD and the counts of days with minimum temperatures less than -23, -19 and -18°C.

For the derived variable estimates the number of annual, downscaled simulations used was 396 (9 models \* 2 downscaling methods \* 2 rcp scenarios \* 11 years = 396 simulation years per projection period).

Ten sample sites were randomly selected from the climate stations data sets and these locations (Figure 1) were used to examine the distributions of derived variable values and to test the fit of selected distributions to data sets from each of these sites. To test the distributions the values for all raster layers in a data set were extracted at each sample site (using the latitude and longitude coordinates of the site). These extracted datasets were then fit to various distributions to identify the most appropriate distribution for the entire dataset.

---

<sup>4</sup> These are the only variables PCIC have made available in statistically downscaled form.

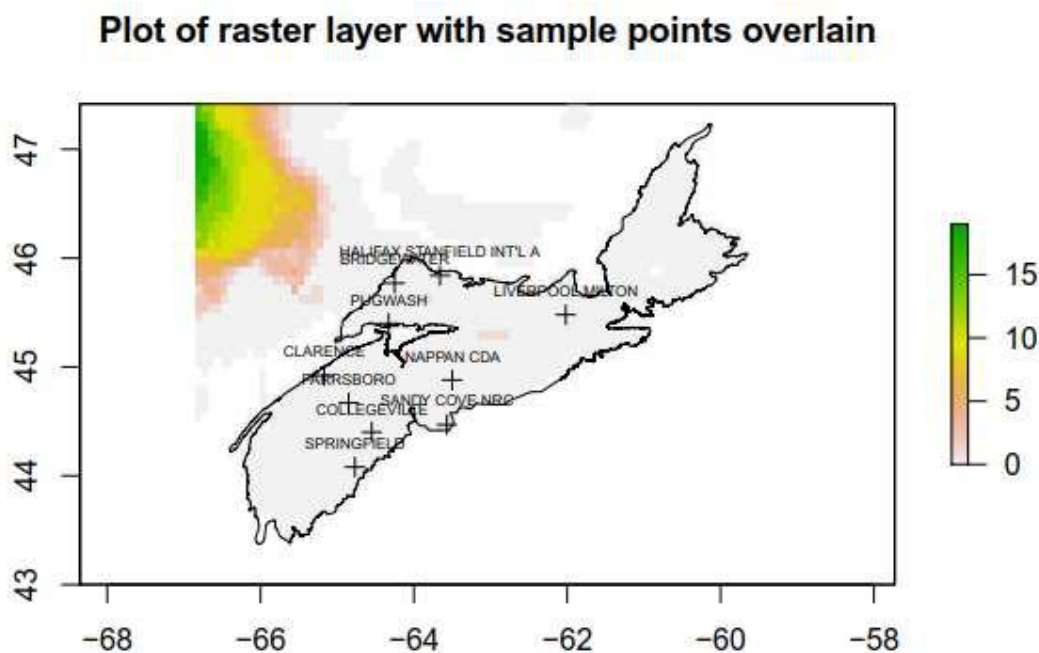


*Figure 1. Map of sample points used for examination of distributional assumptions.*

#### *Count of days exceeding thresholds*

Counts of the number of days that exceeded each of the thresholds  $>0$ ,  $<-23$ ,  $<-19$ ,  $<-18^{\circ}\text{C}$ ) were derived in the following manner:

To estimate the number of days with the minimum daily temperature  $> 0^{\circ}\text{C}$  the tasmin data set was used and for each day in each year of the projection period every grid cell in a map was assigned a value of 1 if the minimum temperature exceeded  $0^{\circ}\text{C}$  and 0 otherwise. Then the values in each cell were simply summed for each year of the projection period for each cell to derive the count of days exceeding  $0^{\circ}\text{C}$  for each year. The result was a grid (i.e. raster map) with the count of days greater than  $0^{\circ}\text{C}$  for each year of the projection period. This result was the estimated number of FFD. A similar approach was used for each of the other thresholds.

Different approaches were used to aggregate the yearly counts to provide estimates for the whole projection period. Prior to aggregating across years, the distributions of values for 10 sample sites were examined and for each site the data were fit to several distributions (normal, lognormal, gamma, Poisson, negative binomial) appropriate for the data. The resulting fits were examined using quantile-quantile plots and plots of the cumulative density functions (empirical versus theoretical). Based on examination of these plots, as well as theoretical considerations, the following distributions were selected for the threshold values:

For the FFD (counts of days  $> 0$ ) estimates, the gamma distribution proved a better fit than the Poisson and hence was used as the distributional basis for these results. For each

projection period maps of seven parameters for FFD were developed and provided as separate raster layers in the delivered geotiff:

- 1) shape parameter ( $k$ ) of gamma distribution fit to the data in each cell of the raster stack
- 2) rate parameter ( $\beta$ ) of gamma distribution
- 3) estimated mean of the distribution using  $\text{mean} = \text{shape} / \text{rate}$
- 4) sd of the shape parameter estimate
- 5) sd of the rate parameter estimate
- 6) lower limit of the 95%CI of mean
- 7) upper limit for the 95% CI of mean

A climate app was developed, using RStudio's Shiny package (Chang, Cheng, Allaire, Xie, & McPherson, 2017) that provided interactive maps of FFD for each projection period with a slider bar that could be used to select a number of FFD see the resulting probabilities of that number or more of FFD.

For the extreme value thresholds  $<-23$ ,  $-19$  and  $<-18$ ) the negative binomial distribution was used. The data were fit to the negative binomial with two parameters: the size and  $\mu$  or the mean. The results are therefore presented as maps with four layers: the first being the size parameter and the second  $\mu$  (the mean). The third and fourth layers were the standard deviations of the size and mean parameters respectively.

In all cases users have been provided with the actual count data for each year as well as the parameters fit to the selected distributions. As with FFD a web app was developed to enable users to interactively examine threshold counts for each period and look at the probabilities for specific count values in each projection period. Similarly, with the FFD app users could also examine the relative change in the mean for each projection period relative to the baseline of 1970 to 2013.

All processing of data was done in R (R Core Team, 2017) with the majority of the spatial data analyses been done using the R package *raster* (Hijmans, 2017). Data were fit to distributions using the *fitdistrplus* package (Delignette-Muller & Dutang, 2015). Bayesian Network modelling (including tree-augmented Naïve Bayes) was undertaken with the *bnlearn* package (Scutari, 2010). Bayesian regression modelling used the *brms* package (Burkner, 2017), an interface to STAN (Carpenter et al., 2017).

### Growing degree days

GDD were derived for each year and thence for each projection period using a base of 10°C and with the estimation done for April 1<sup>st</sup> to October 31<sup>st</sup> each year. For all GDD estimates, matching<sup>5</sup> tasmin and tasmax data sets for each year were used.

Estimates of GDD for each year of each projection period were derived using the following relationship:

$$GDD_{base\_x} = \begin{cases} 0, & \frac{tmax - tmin}{2} \leq base\_x \\ \sum_{i=1}^n \frac{tmax - tmin}{2} - base\_x, & \frac{tmax - tmin}{2} > base\_x \end{cases}$$

Where:

GDD = growing degree days

*base\_x* = the base used to estimate GDD (either 0 or 10°C)

*tmax* and *tmin* are the daily maximum and minimum temperatures respectively

When aggregating GDD across years for the projection period the best fitting distribution was a gamma distribution. The results for GDD are thus presented as a map with seven layers with the same layer names as described above for FFD.

There is some diversity in how GDD have been estimated. For the production of grapes the concept was proposed by Winkler, Cook, Kliwer, and Lider (1974) and following on from this now classic book the general practice of summing the average daily temperature above a threshold for the period April 1<sup>st</sup> to October 30<sup>th</sup> (in the northern hemisphere) has commonly been used. Different thresholds have been proposed and evaluated (A. K. Parker, De CortÁZar-Atauri, Van Leeuwen, & Chuine, 2011) with 10°C commonly used for grapes, but 5°C or 0°C are also used. Different start and end dates for the accumulation have also been proposed and evaluated (García de Cortázar-Atauri, Brisson, & Gaudillere, 2009; A. Parker et al., 2013; A. K. Parker et al., 2011).

As with the threshold data the GDD projections (for each calculation approach) were provided to users in three forms: firstly, as complete sets of the estimated GDD for each cell for each year; secondly the geotiff of gamma parameters and the mean for the whole period; and thirdly as an interactive app.

---

<sup>5</sup> The same simulation comprising model, downscaling and scenario were used for tasmin as for tasmax.

## Overview of the projection data

### Distributional assumptions

As noted in the methods section of the report GDD results were fit to gamma distributions to enable better approximation of the skewed distributions for these results. Two hundred distributional test plots were produced but only a few are presented here to illustrate the distributional decisions that were made for each variable.

### Growing degree days (GDD)

GDD results were generally well represented by gamma distributions (see for example Figure 2, Figure 3).

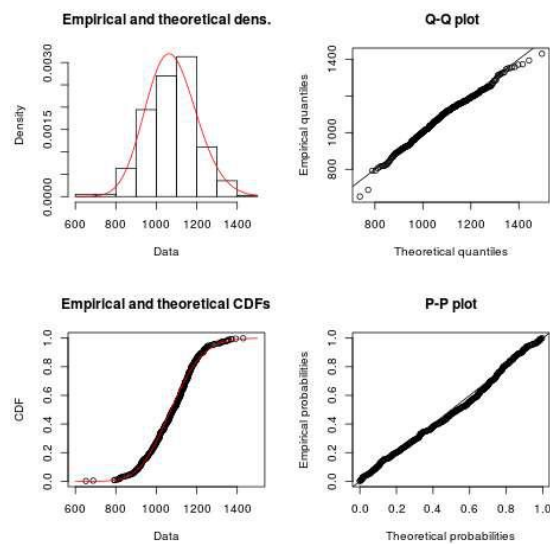


*Figure 2. GDD estimates for base 10, April to October 2030 to 2040 (i.e. centred on 2035) for Bridgewater, fit to gamma distribution.*

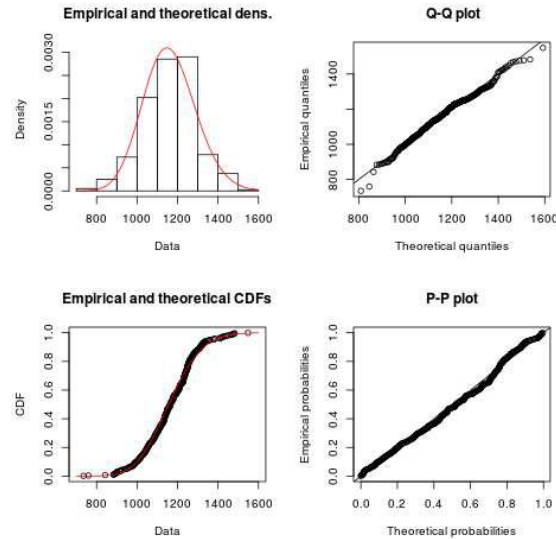


Figure 3. GDD estimates for base 10, April to October 2030 to 2040 (i.e. centred on 2035) for Halifax International Airport, fit to gamma distribution.

### Counts of days exceeding thresholds

The counts of frost free days (estimated for a base of 0°C) were fit to gamma distributions (see examples in Figure 4, **Error! Reference source not found.**, Figure 5, **Error! Reference source not found.**) whilst the counts of days exceeding extreme value thresholds (i.e. for days less than -23, -19 and -18°C) were modelled as negative binomial distributions (Figure 7 to **Error! Reference source not found.**). For each of the threshold estimates only a few of the total set of distributional plots are shown by way of illustration.

Frost free days were well represented by the gamma distribution. For the counts of days less than -18, -19 or -23 °C the negative binomial distribution was a good fit.

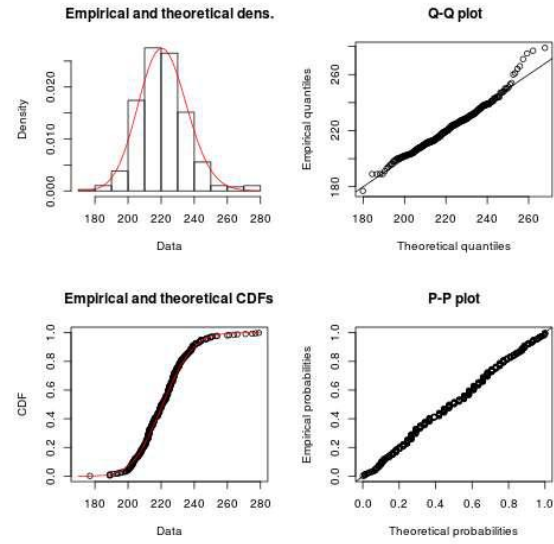


Figure 4. Count of FFD (using base 0) per year for the period 2020 to 2030 (i.e. centred on 2025) for Liverpool Milton, fit to Gamma distribution.

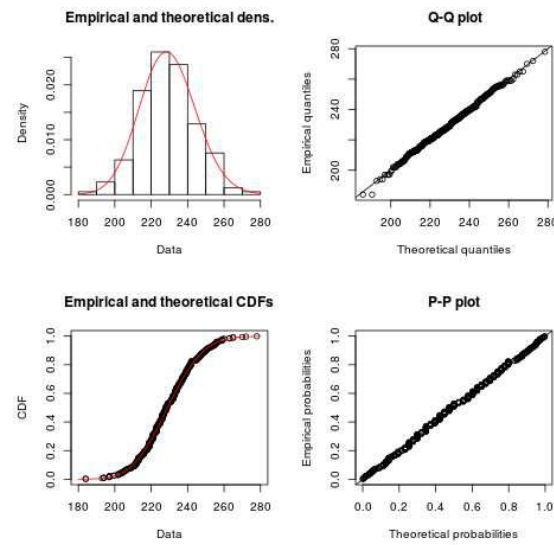


Figure 5. Count of FFD (using base 0) per year for the period 2030 to 2040 (i.e. centred on 2035) for Liverpool Milton, fit to gamma distribution.



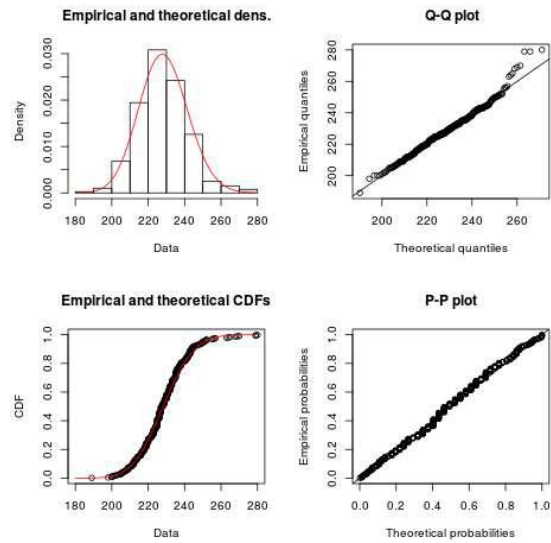


Figure 6. Count of FFD (using base 0) per year for the period 2020 to 2030 (i.e. centred on 2025) for Halifax International Airport, fit to gamma distribution.

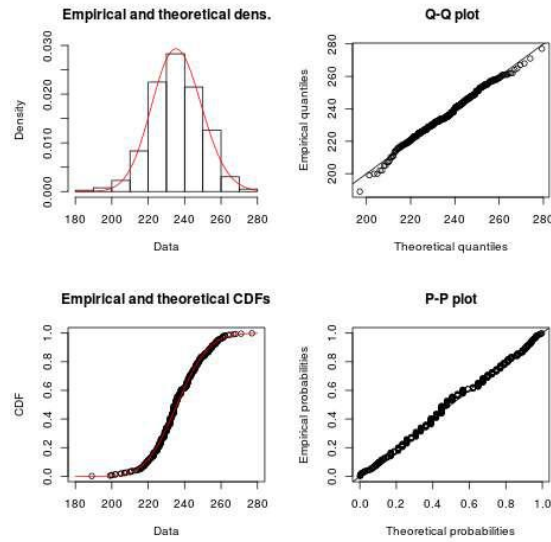


Figure 7. Count of FFD (using base 0) per year for the period 2030 to 2040 (i.e. centred on 2035) for Halifax International Airport, fit to gamma distribution.

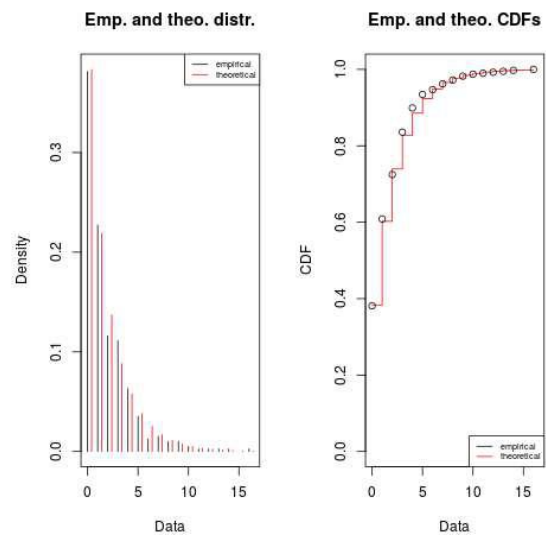


Figure 8. Count of days less than  $-23^{\circ}\text{C}$  per year for the period 2020 to 2030 (i.e. centred on 2025) for Bridgewater, fit to negative binomial distribution.

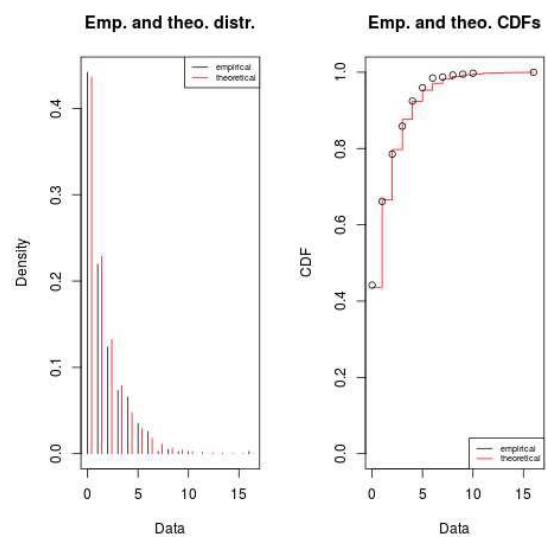


Figure 9. Count of days less than  $-23^{\circ}\text{C}$  per year for the period 2030 to 2040 (i.e. centred on 2035) for Bridgewater, fit to negative binomial distribution.

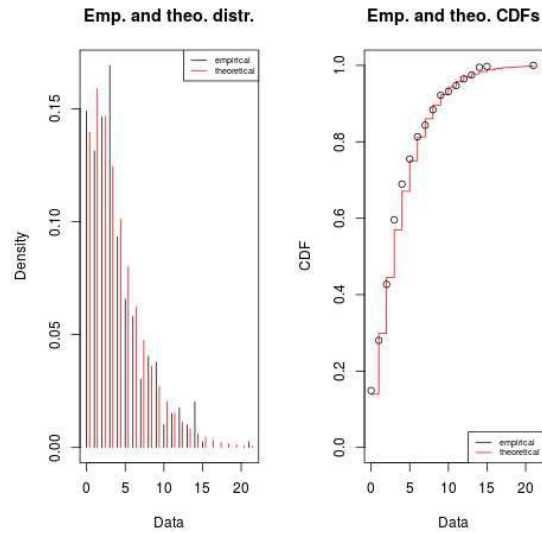


Figure 10. Count of days less than  $-18^{\circ}\text{C}$  per year for the period 2030 to 2040 (i.e. centred on 2035) for Collegeville, fit to negative binomial distribution.

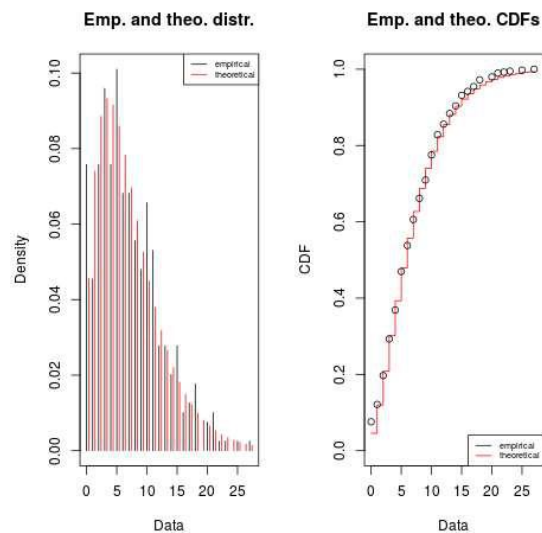


Figure 11. Count of days less than  $-18^{\circ}\text{C}$  per year for the period 2030 to 2040 (i.e. centred on 2035) for Halifax International Airport, fit to negative binomial distribution.

## Mapping of key variables and change relative to baseline

In this section the results of projections of derived variables are presented and compared to the 1970 to 2013 baseline. Growing degree days (GDD), frost free days (FFD), days less than  $-19^{\circ}\text{C}$  and days less than  $-23^{\circ}\text{C}$  are each presented in separate sections. In each section the results of simulated projections are first compared to the baseline results derived from the NRCan modelled data before the projection data are presented. For GDD each of the projections (2020, 2025, 2030, 2035 and 2050) are presented but for the other sections (to simplify the presentation) just the 2025, 2035 and 2050 projections are presented.

## Growing degree days

The downscaled GCM data were slightly higher (mean 1.03, std 0.01) relative to NRCan modelled data but this difference is well within the 95% confidence intervals of the estimation of GDD for the baseline (Figure 12). All comparisons are hereafter carried out with the downscaled modelled baseline.

GDD increased by between 14 and 18% between the baseline period (1970 to 2013) and the 2020 projection period with the greatest increases along the western coastline and northern Cape Breton Island (Figure 13). By 2025 GDD increases by 17 to 26%, again with the greatest increases along the western coastline but also along the eastern coastline (Figure 14). By the 2030 projection period GDD increased by 20 to 28%, again particularly along the western, south-western and eastern coastlines but also on the northern tip of Cape Breton Island (Figure 15). GDD had increased by 22 to 30% (relative to 1970 to 2013) in the 2035 projection period (Figure 16) and by between 30 to over 40% by 2050 (Figure 17).

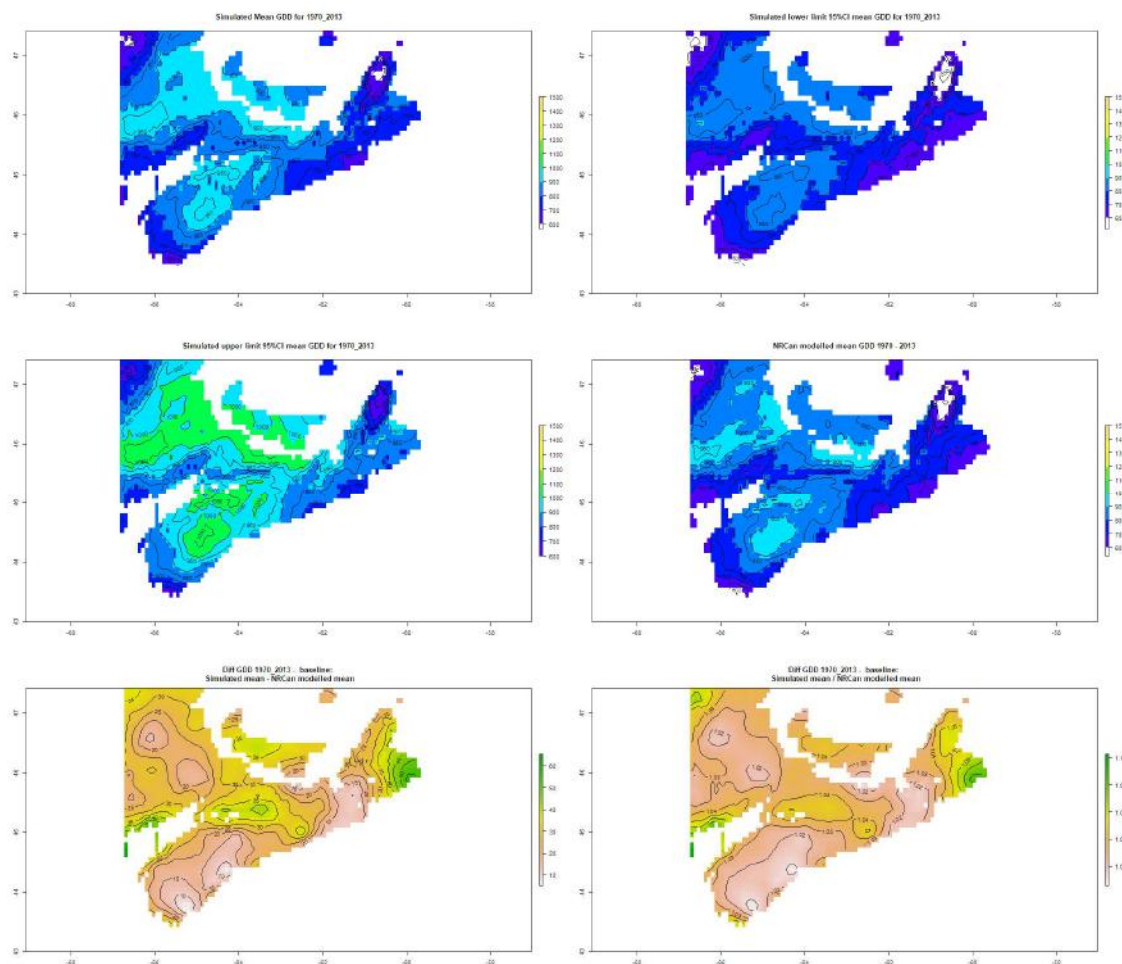
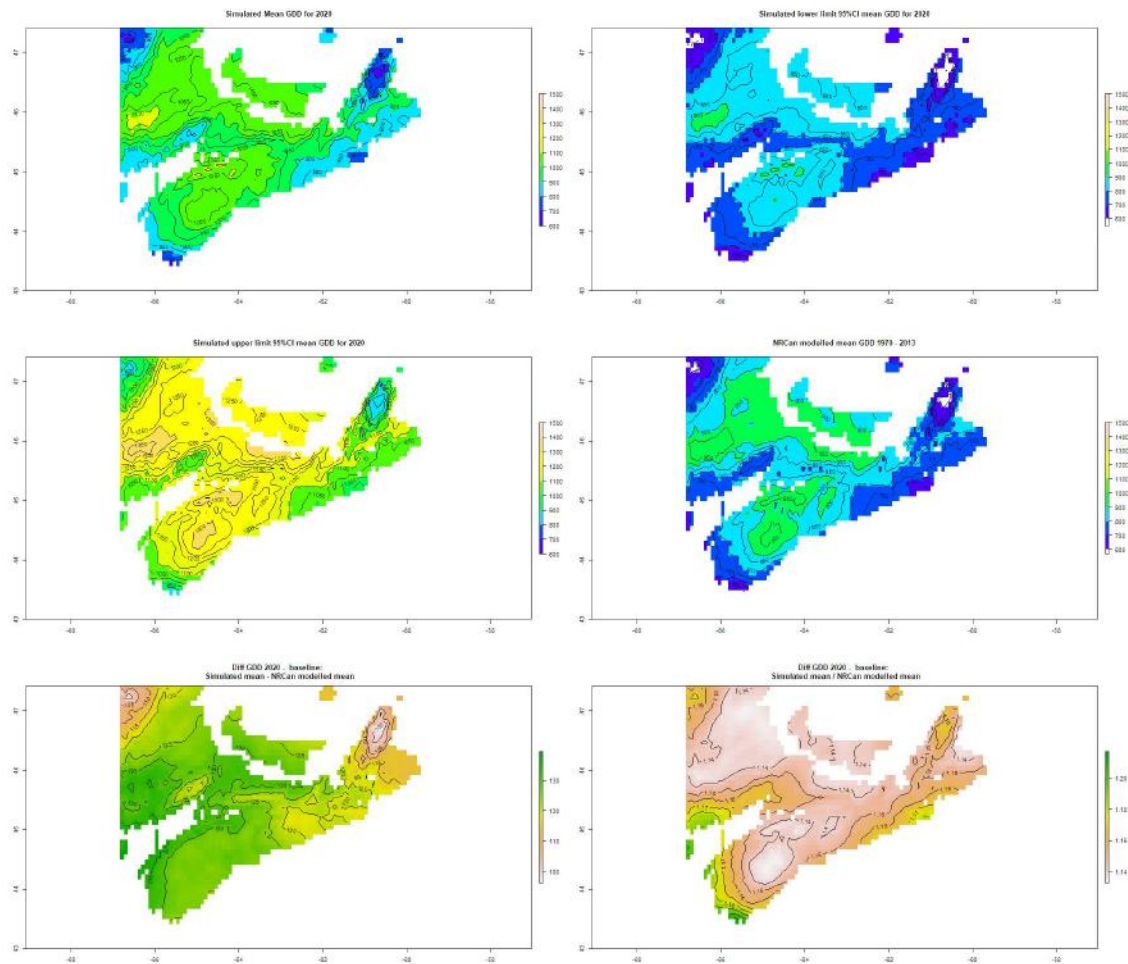


Figure 12. GDD 1970 to 2013. Top left: simulated mean GDD; top right, lower limit of the 95% CI for the mean; centre left, upper limit to the 95% CI; centre right NRCan modelled mean;

*bottom left, NRCan mean minus simulated mean; bottom right, NRCan mean / simulated mean.*

Uncertainty in the projections (as measured by the width of the 95% confidence intervals) showed only minor change through time, with slightly wider CI's in 2050 relative to 2020 but there was no spatial pattern evident in the uncertainty (Figure 18).



*Figure 13. Maps of changes in GDD (relative to 1970 to 2013 baseline) for 2020 projection period. Top left: simulated mean GDD; top right, lower limit of the 95% CI for the mean; centre left, upper limit to the 95% CI; centre right baseline (modelled) mean for 1970 to 2013; bottom left, baseline mean minus simulated mean; bottom right, baseline mean / simulated mean.*

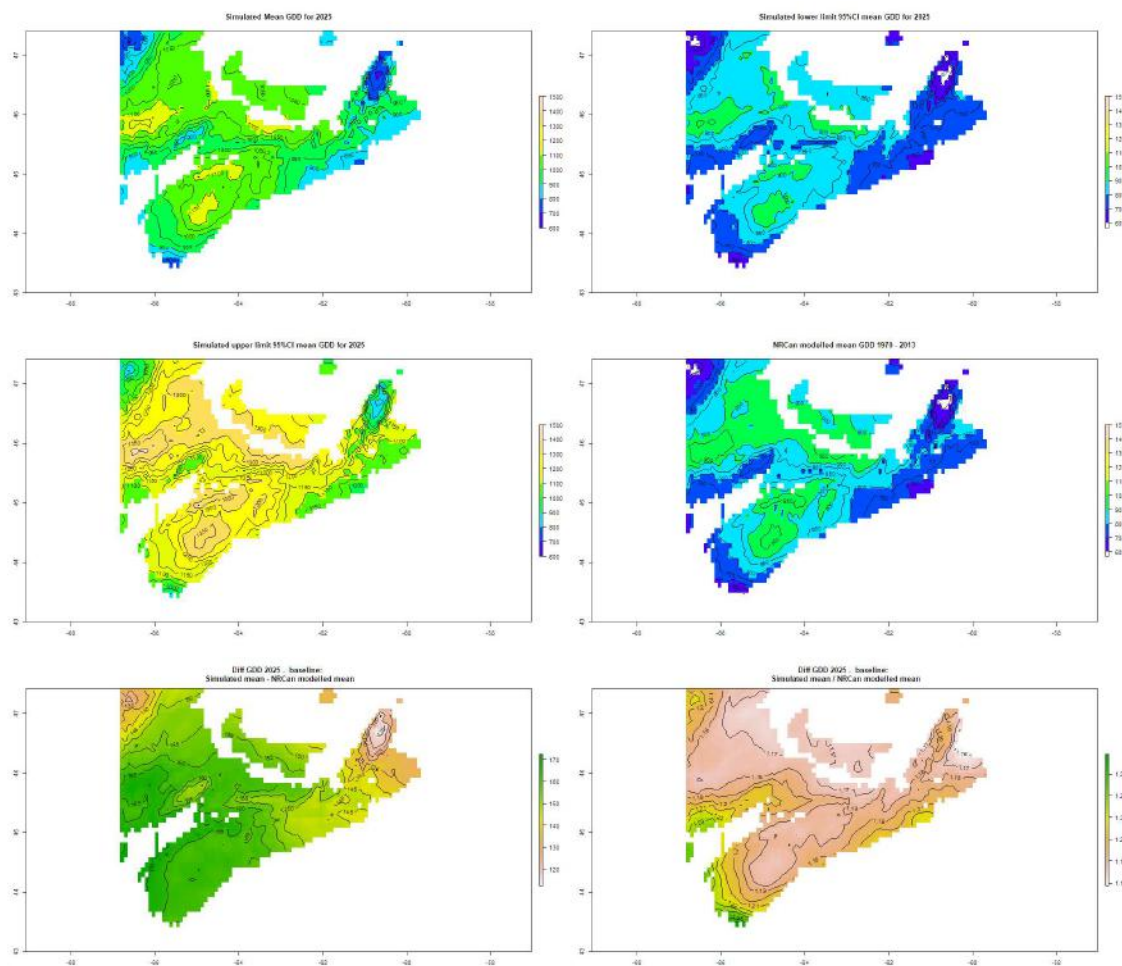


Figure 14. Maps of changes in GDD (relative to 1970 to 2013 baseline) for 2025 projection period. Top left: simulated mean GDD; top right, lower limit of the 95% CI for the mean; centre left, upper limit to the 95% CI; centre right baseline (modelled) mean for 1970 to 2013; bottom left, baseline mean minus simulated mean; bottom right, baseline mean / simulated mean.



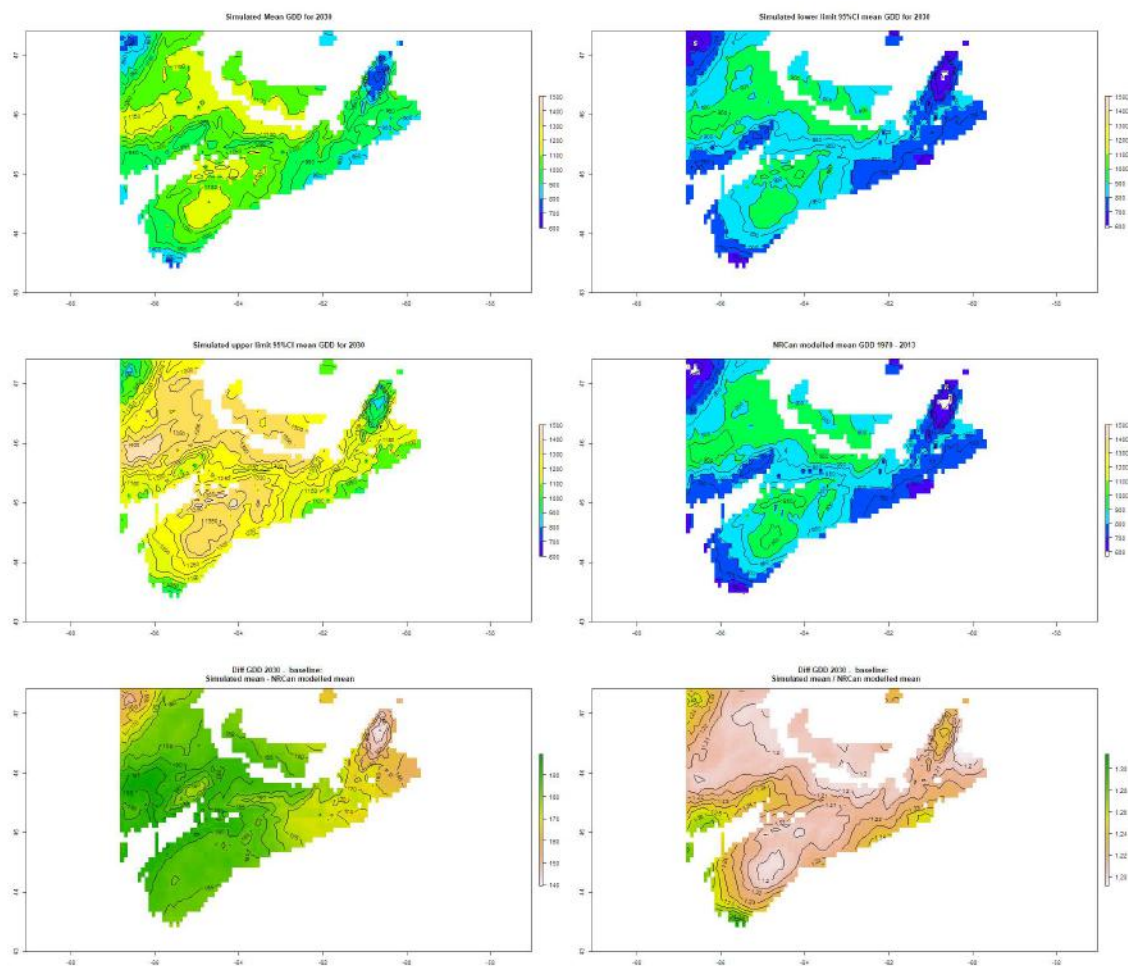


Figure 15. Maps of changes in GDD (relative to 1970 to 2013 baseline) for 2030 projection period. Top left: simulated mean GDD; top right, lower limit of the 95% CI for the mean; centre left, upper limit to the 95% CI; centre right baseline (modelled) mean for 1970 to 2013; bottom left, baseline mean minus simulated mean; bottom right, baseline mean / simulated mean.

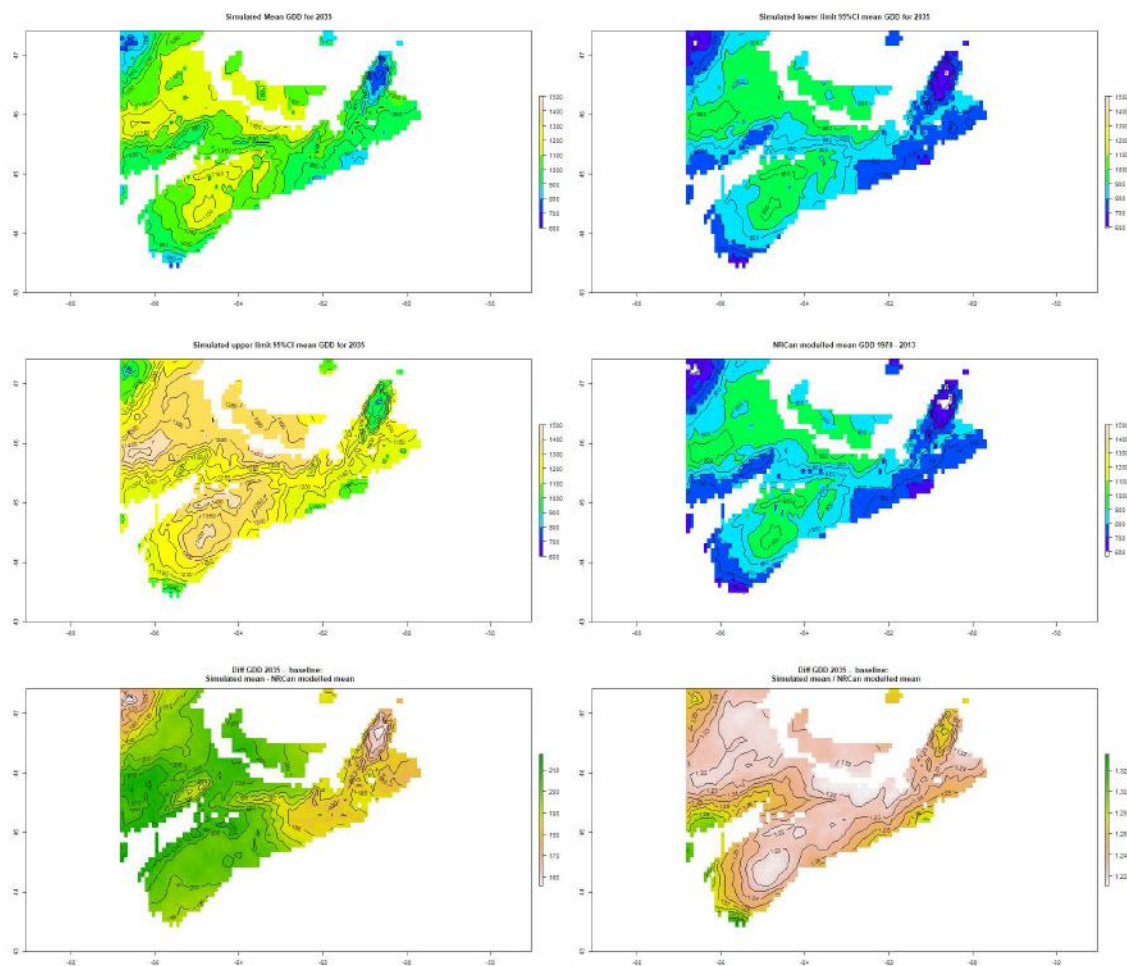


Figure 16. Maps of changes in GDD (relative to 1970 to 2013 baseline) for 2035 projection period. Top left: simulated mean GDD; top right, lower limit of the 95% CI for the mean; centre left, upper limit to the 95% CI; centre right baseline (modelled) mean for 1970 to 2013; bottom left, baseline mean minus simulated mean; bottom right, baseline mean / simulated mean.



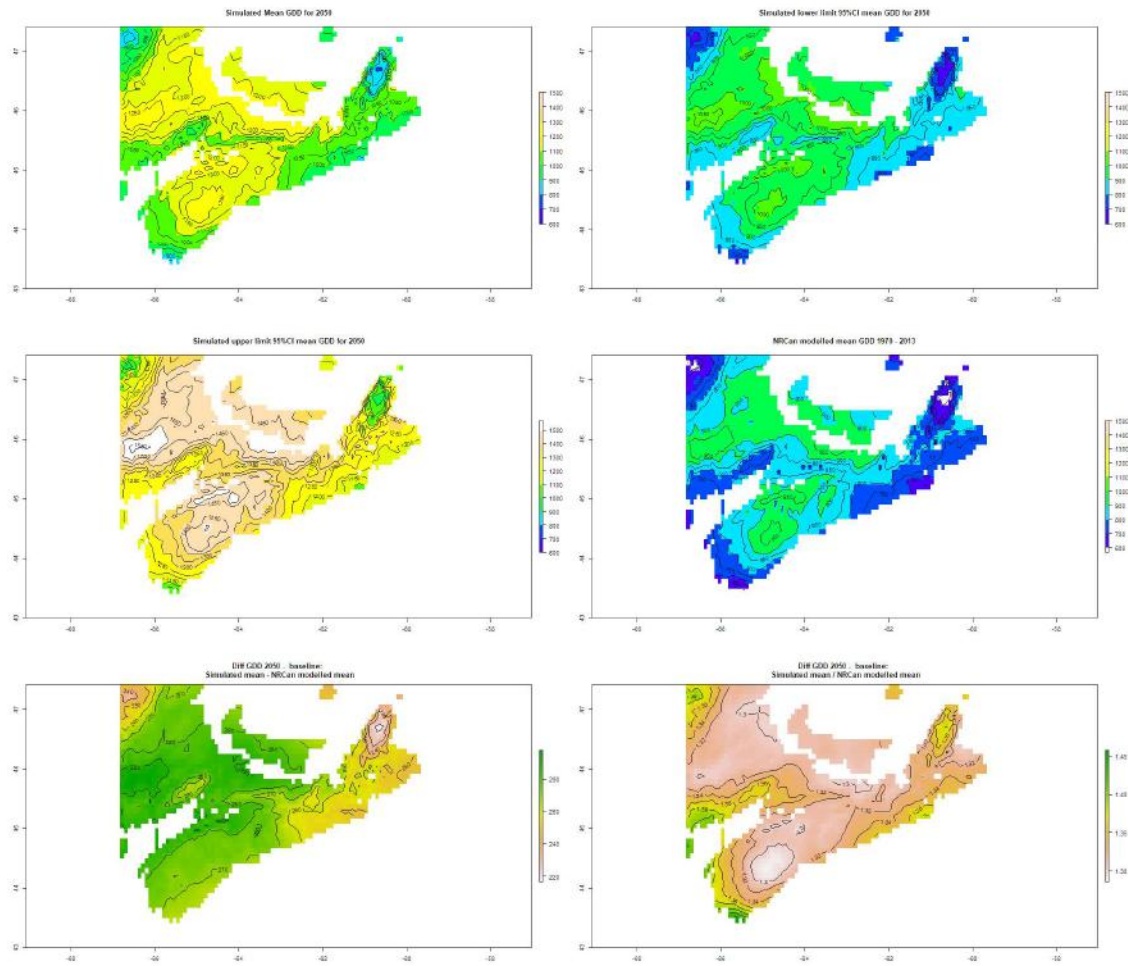


Figure 17. Maps of changes in GDD (relative to 1970 to 2013 baseline) for 2050 projection period. Top left: simulated mean GDD; top right, lower limit of the 95% CI for the mean; centre left, upper limit to the 95% CI; centre right baseline (modelled) mean for 1970 to 2013; bottom left, baseline mean minus simulated mean; bottom right, baseline mean / simulated mean.

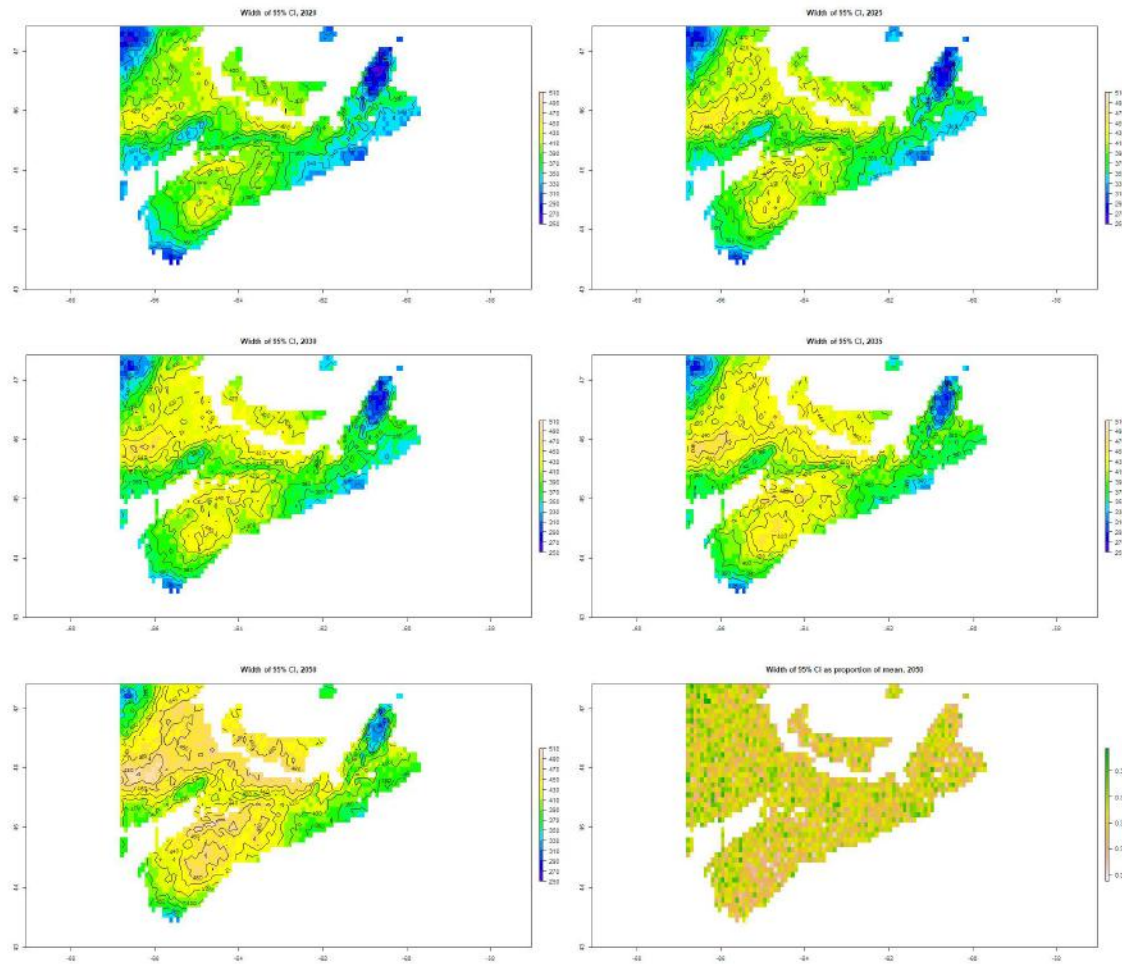


Figure 18. Maps of 95% CI widths (upper – lower) for each projection period with the width as a proportion of the mean for 2050 at bottom right.

### Frost free days (FFD)

The frost-free period was projected to increase by between 16 and 22 days (7 to 10%) by 2025 (Figure 19), by 22 to 32 days (9 to 14%) by 2035 (Figure 20) and by 30 to 38 days (12 to 18%) by 2050 (Figure 21). Three “bands” (running approximately NW to SE) of notable increases in the frost-free period were evident, one roughly between Digby and Liverpool, one between Tatamagouche and Beaver Harbour on the east coast and one in Cape Breton from roughly Inverness to roughly the Stillwaters Wilderness area.

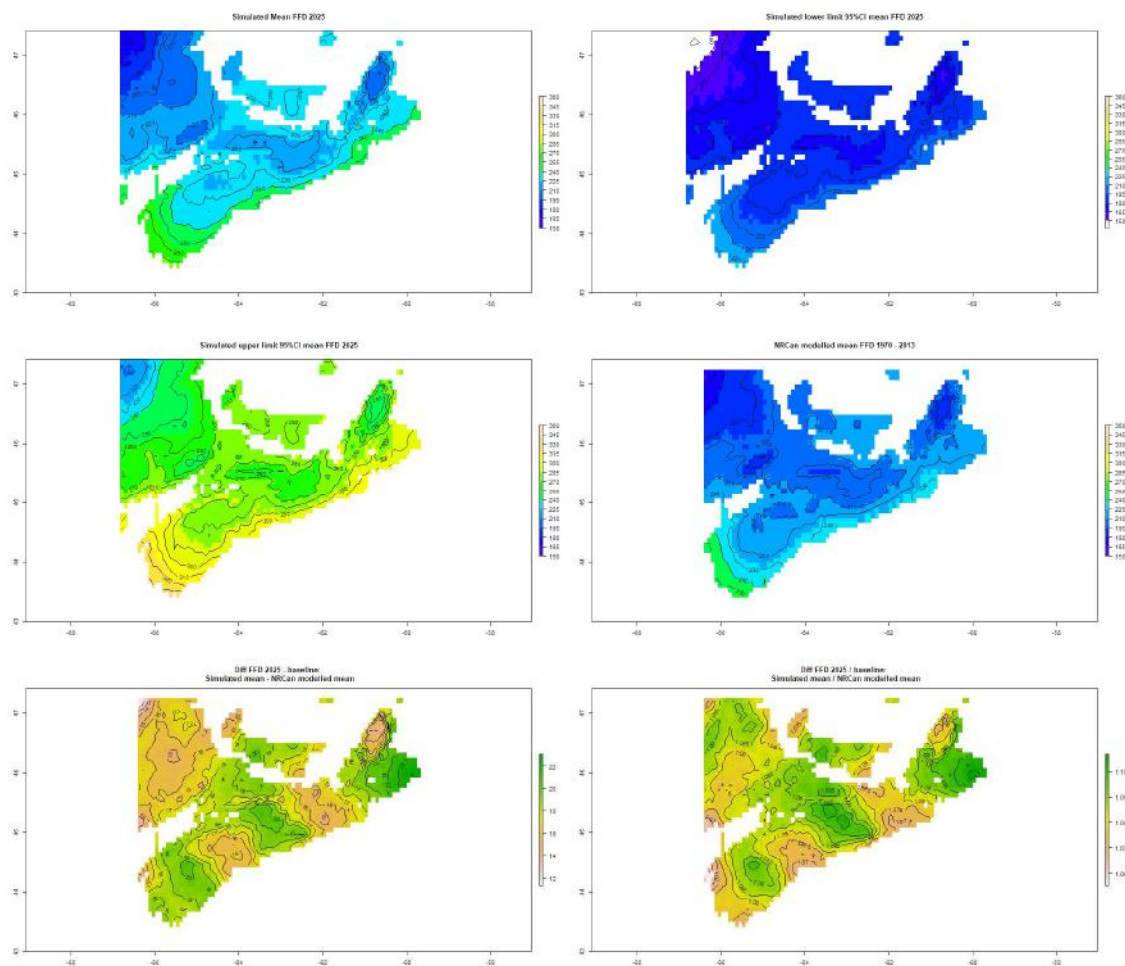


Figure 19. Maps of changes in frost free days (FFD) relative to 1970 to 2013 baseline for 2025 projection period. Top left: simulated mean FFD; top right, lower limit of the 95% CI for the mean; centre left, upper limit to the 95% CI; centre right baseline (modelled) mean FFD for 1970 to 2013; bottom left, baseline mean minus simulated mean; bottom right, baseline mean / simulated mean.

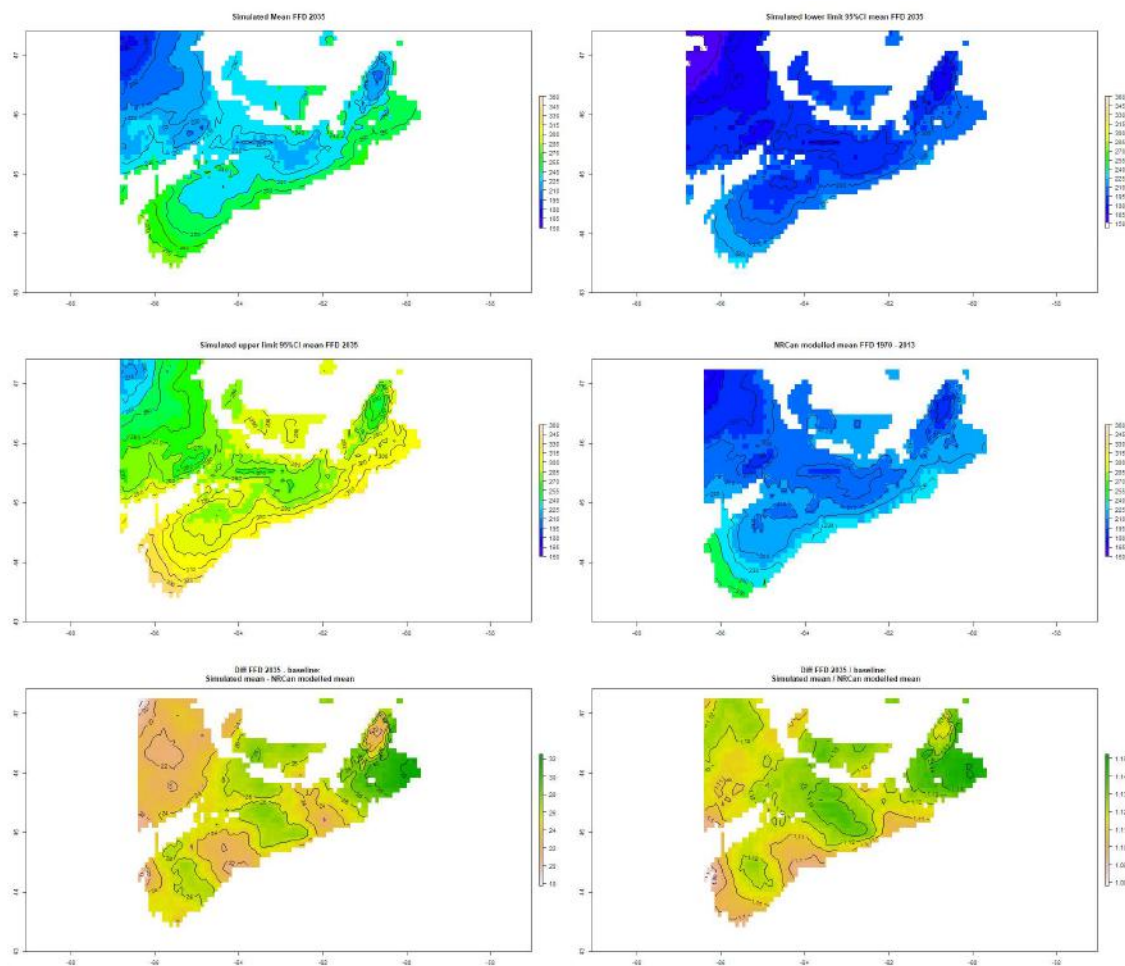


Figure 20. Maps of changes in frost free days (FFD) relative to 1970 to 2013 baseline for the 2035 projection period. Top left: simulated mean FFD; top right, lower limit of the 95% CI for the mean; centre left, upper limit to the 95% CI; centre right baseline (modelled) mean FFD for 1970 to 2013; bottom left, baseline mean minus simulated mean; bottom right, baseline mean / simulated mean.

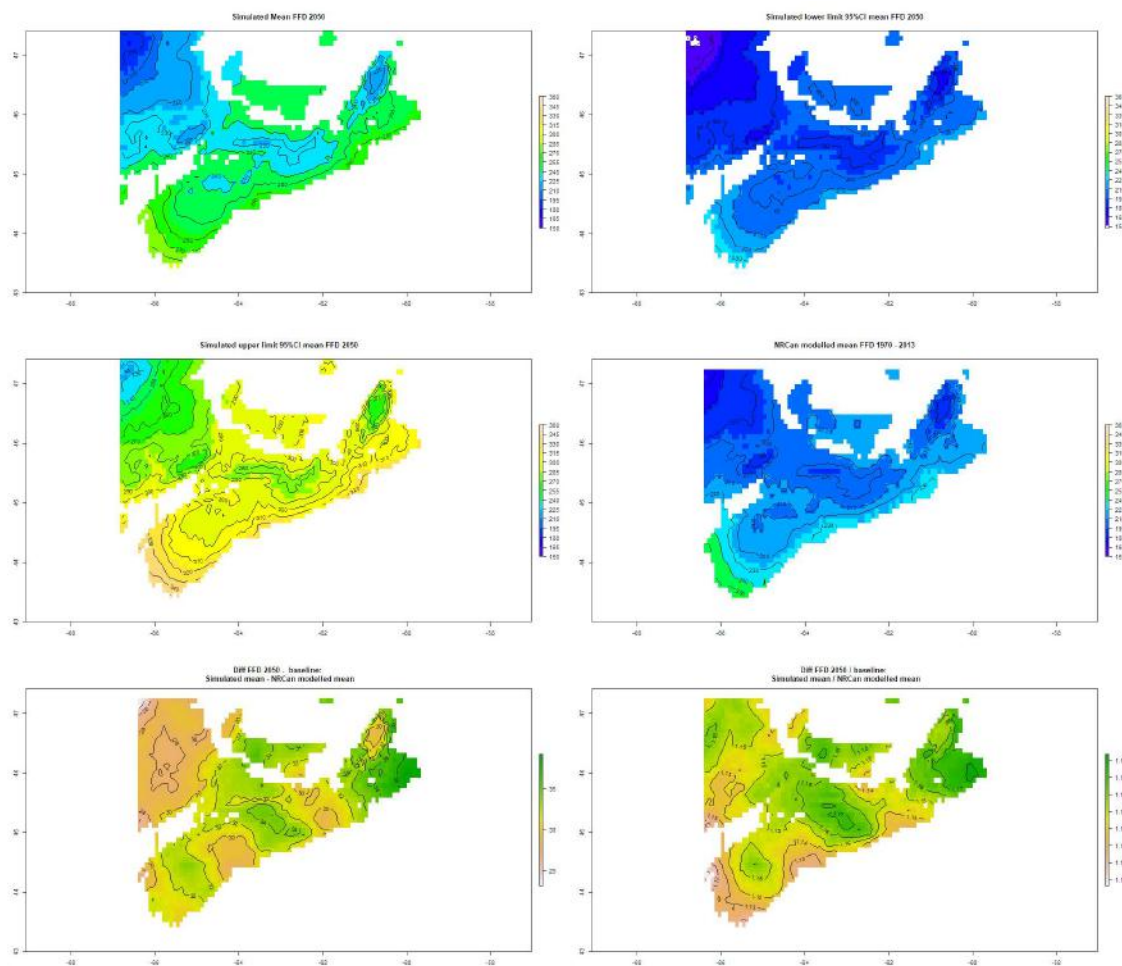


Figure 21. Maps of changes in frost free days (FFD) relative to 1970 to 2013 baseline for the 2050 projection period. Top left: simulated mean FFD; top right, lower limit of the 95% CI for the mean; centre left, upper limit to the 95% CI; centre right baseline (modelled) mean FFD for 1970 to 2013; bottom left, baseline mean minus simulated mean; bottom right, baseline mean / simulated mean.

#### Days with minimum temperature less than -19°C<sup>6</sup>

The projected number of days with minimum temperatures less than -19°C (DL19) for the baseline period (1970 to 2013) varied from about +10% to -15% relative to the NRCan modelled data with the greatest differences along the western coastline (Figure 22).

Using the simulated baseline as a reference the DL19 number of was projected to decrease by between one and four days (45 to 70%) by the 2025 period compared to the 1970 to 2013 baseline period (Figure 23). Thereafter the DL19 steadily decreased to only between 15 and 30% of their baseline number by 2050 (Figure 24, Figure 25). The greatest decreases were projected to occur along the western and north eastern coastlines.

<sup>6</sup> The results for days less than -18°C are not shown as they are very close to the results for -19°C.



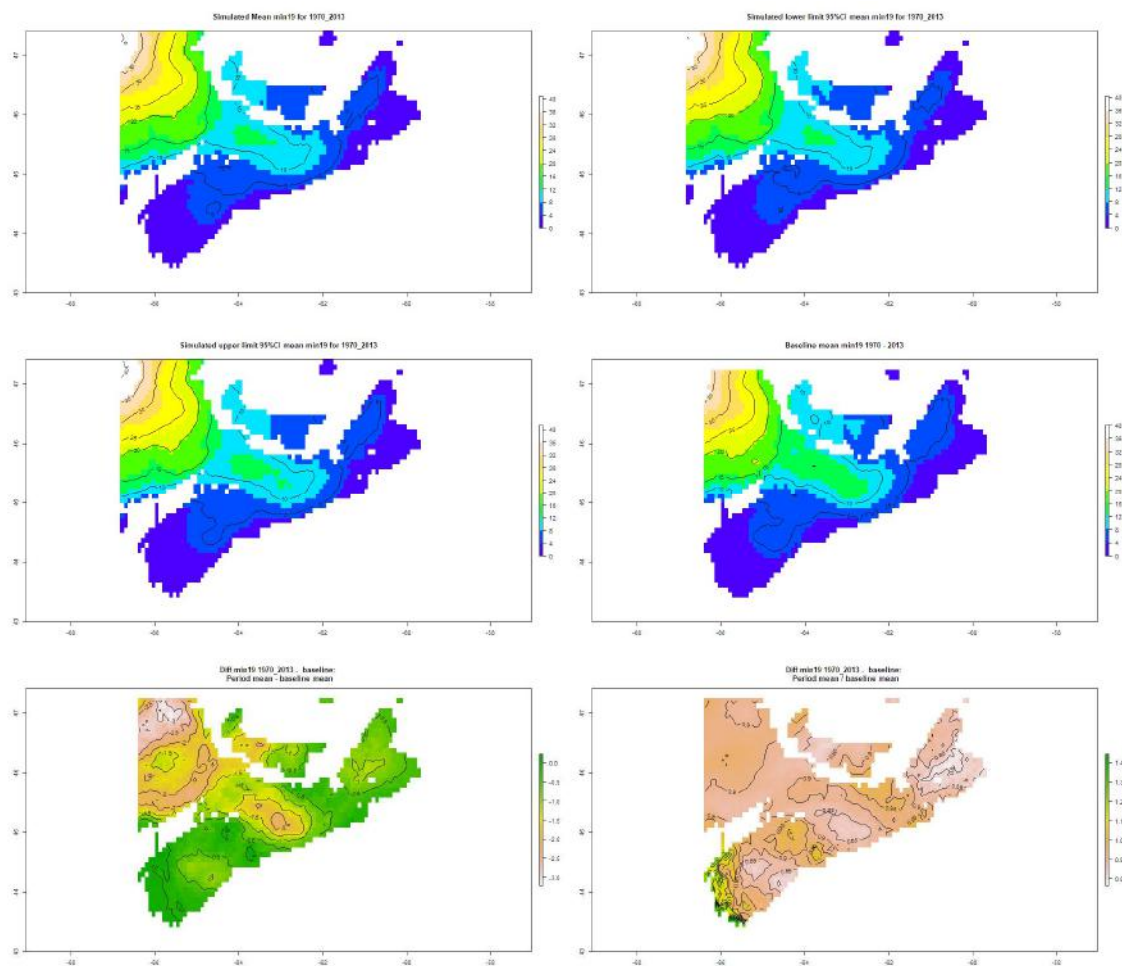


Figure 22. Comparison of simulated versus NRCAN modelled days with a minimum temperature less than  $-19^{\circ}\text{C}$  (DL19) for the 1970 to 2013 period. Top left: simulated mean DL19; top right, lower limit of the 95% CI for the mean; centre left, upper limit to the 95% CI; centre right NRCAN (modelled) mean DL19 for 1970 to 2013; bottom left, baseline mean minus simulated mean; bottom right, baseline mean / simulated mean.

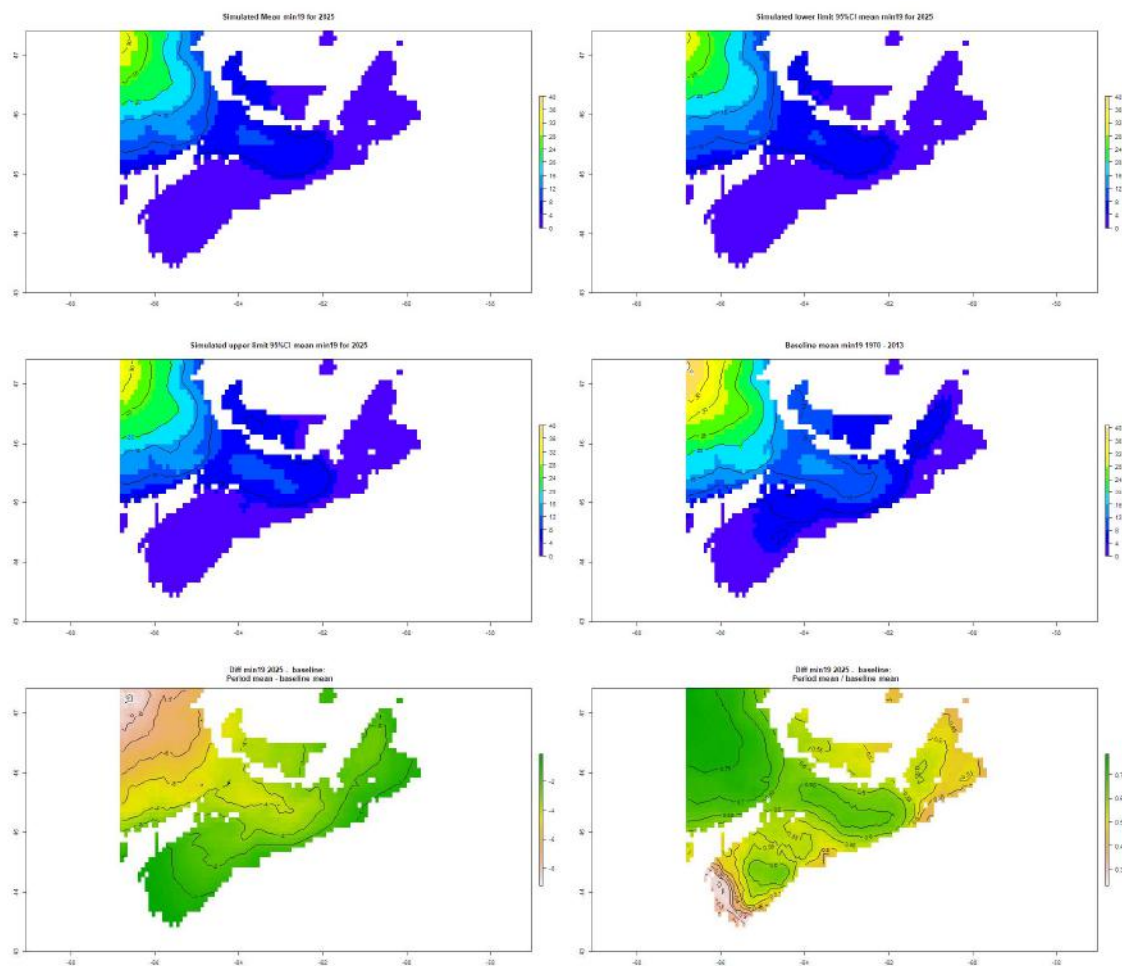


Figure 23. Maps of changes in the number of days less than  $-19^{\circ}\text{C}$  (DL19) relative to the simulated 1970 to 2013 baseline for the 2025 projection period. Top left: simulated mean DL19; top right, lower limit of the 95% CI for the mean; centre left, upper limit to the 95% CI; centre right baseline (modelled) mean DL19 for 1970 to 2013; bottom left, baseline mean minus simulated mean; bottom right, baseline mean / simulated mean.

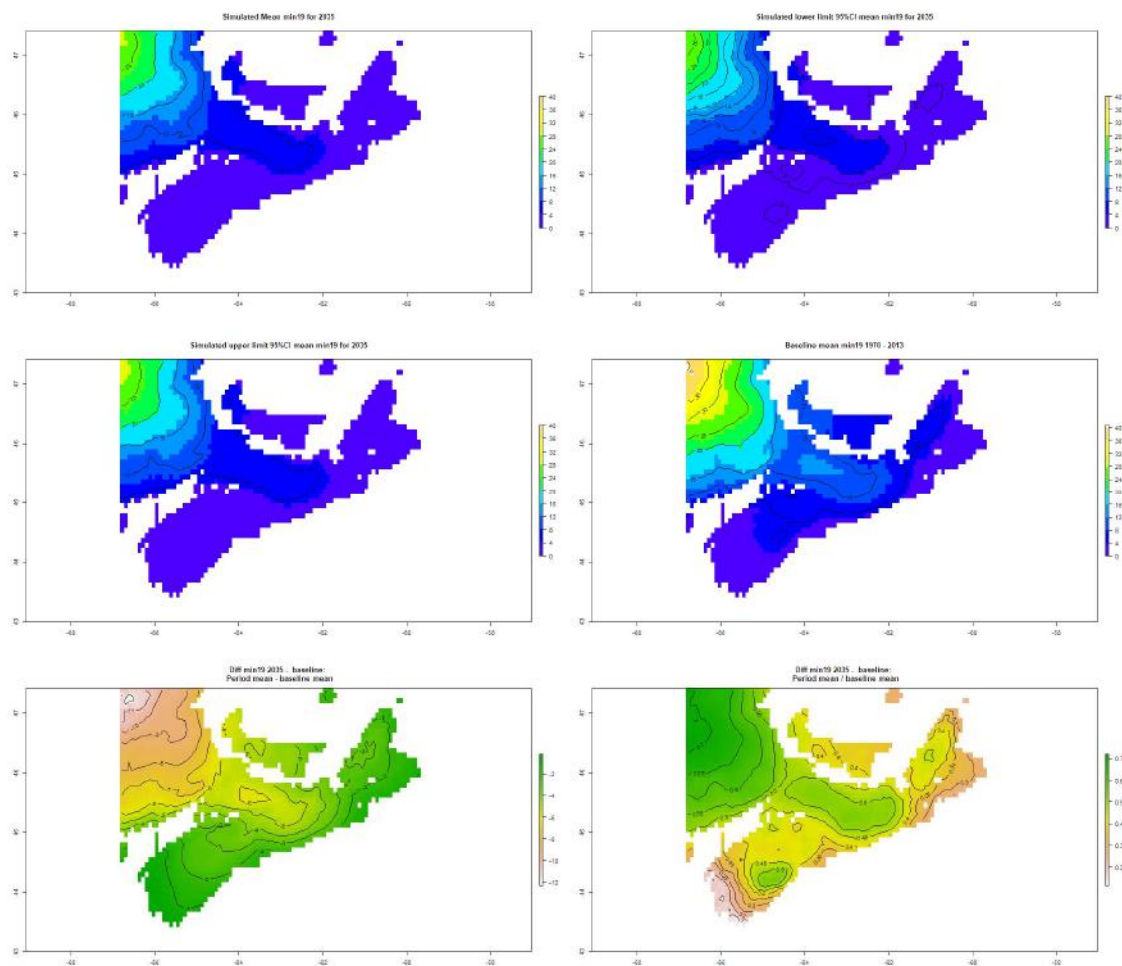


Figure 24. Maps of changes in the number of days less than  $-19^{\circ}\text{C}$  (DL19) relative to the simulated 1970 to 2013 baseline for the 2035 projection period. Top left: simulated mean DL19; top right, lower limit of the 95% CI for the mean; centre left, upper limit to the 95% CI; centre right baseline (modelled) mean DL19 for 1970 to 2013; bottom left, baseline mean minus simulated mean; bottom right, baseline mean / simulated mean.



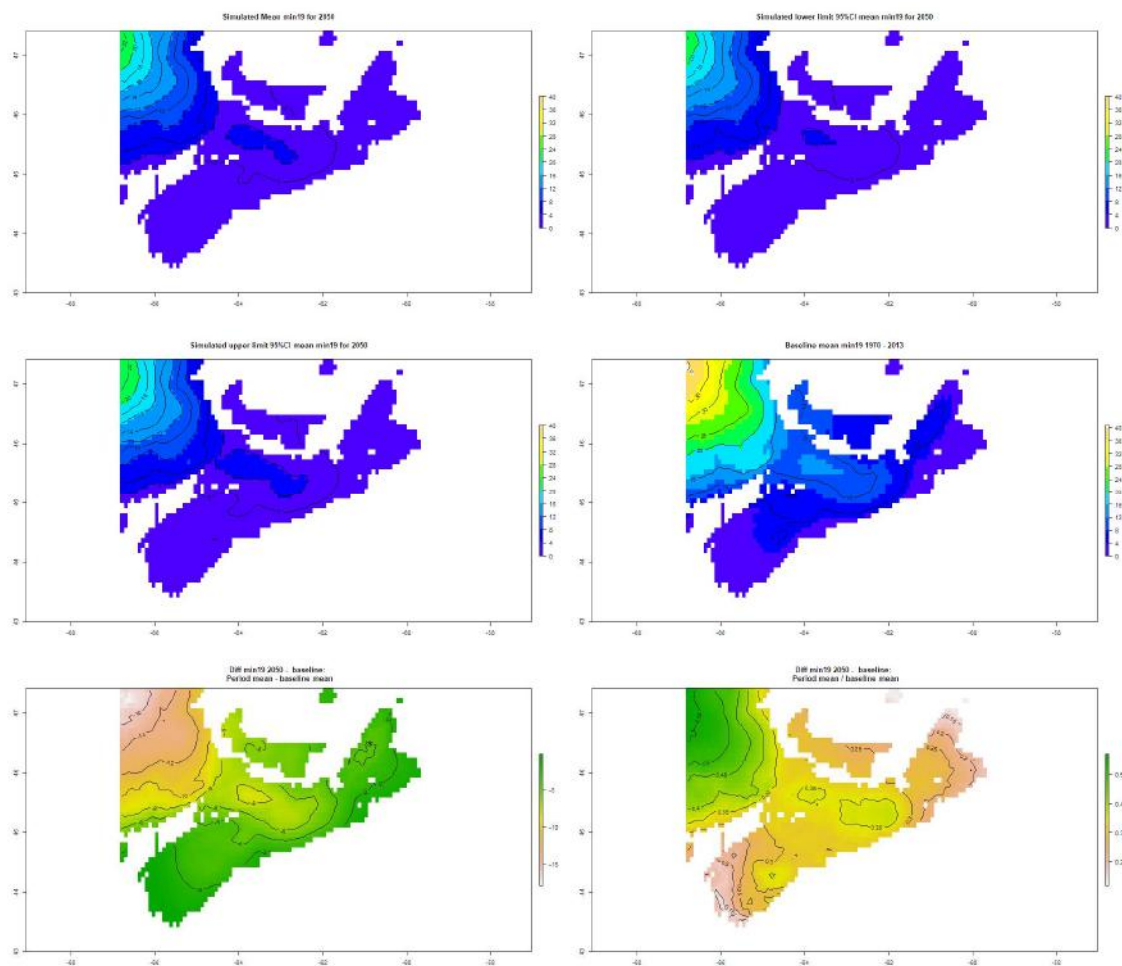


Figure 25. Maps of changes in the number of days less than  $-19^{\circ}\text{C}$  (DL19) relative to the simulated 1970 to 2013 baseline for the 2050 projection period. Top left: simulated mean DL19; top right, lower limit of the 95% CI for the mean; centre left, upper limit to the 95% CI; centre right baseline (modelled) mean DL19 for 1970 to 2013; bottom left, baseline mean minus simulated mean; bottom right, baseline mean / simulated mean.

#### Days with minimum temperature less than $-23^{\circ}\text{C}$

The number of days with minimum temperatures less than  $-23^{\circ}\text{C}$  (DL23) in the simulations for the baseline period (1970 to 2013) was very similar to the values derived from the NRCan modelled data (Figure 26). DL23 was projected to decrease by less than a day to one day by the 2050 period compared to the 2020 period (Figure 22).

Compared to the 1970 to 2013 baseline the DL23 were projected to decrease by between 65 and 100% by 2050 with the greatest decreases likely to occur along the western and north eastern coastlines (Figure 29). For most of Nova Scotia there is projected to be less than one day of minimum daily temperatures less than  $-23^{\circ}\text{C}$  by 2035 (Figure 28).

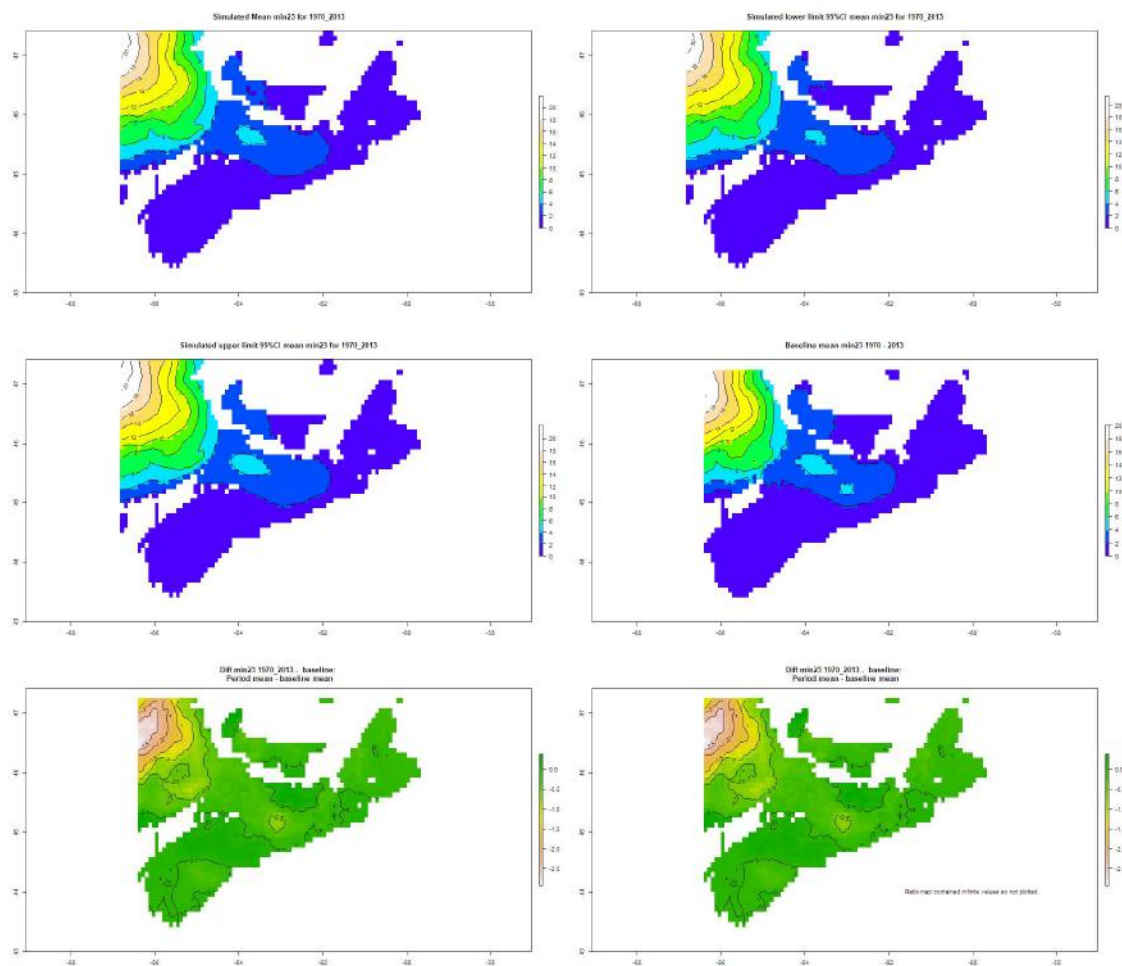


Figure 26. Comparison of simulated versus NRCAN modelled days with a minimum temperature less than -23°C (DL23) for the 1970 to 2013 period. Top left: simulated mean DL23; top right, lower limit of the 95% CI for the mean; centre left, upper limit to the 95% CI; centre right NRCAN (modelled) mean DL23 for 1970 to 2013; bottom left, baseline mean minus simulated mean; bottom right, baseline mean / simulated mean.

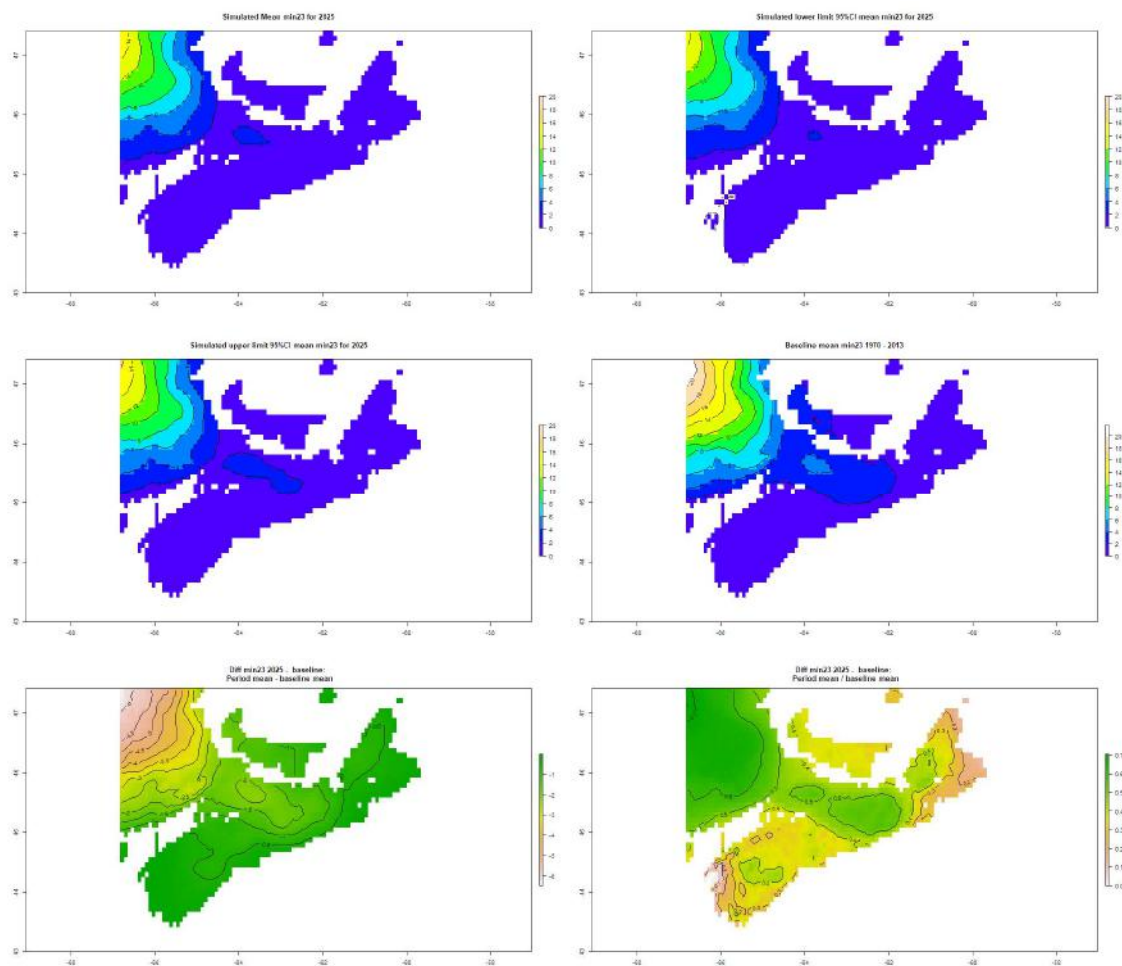


Figure 27. Maps of changes in the number of days less than  $-23^{\circ}\text{C}$  (DL23) relative to the simulated 1970 to 2013 baseline for the 2025 projection period. Top left: simulated mean DL23; top right, lower limit of the 95% CI for the mean; centre left, upper limit to the 95% CI; centre right baseline (modelled) mean DL23 for 1970 to 2013; bottom left, baseline mean minus simulated mean; bottom right, baseline mean / simulated mean.

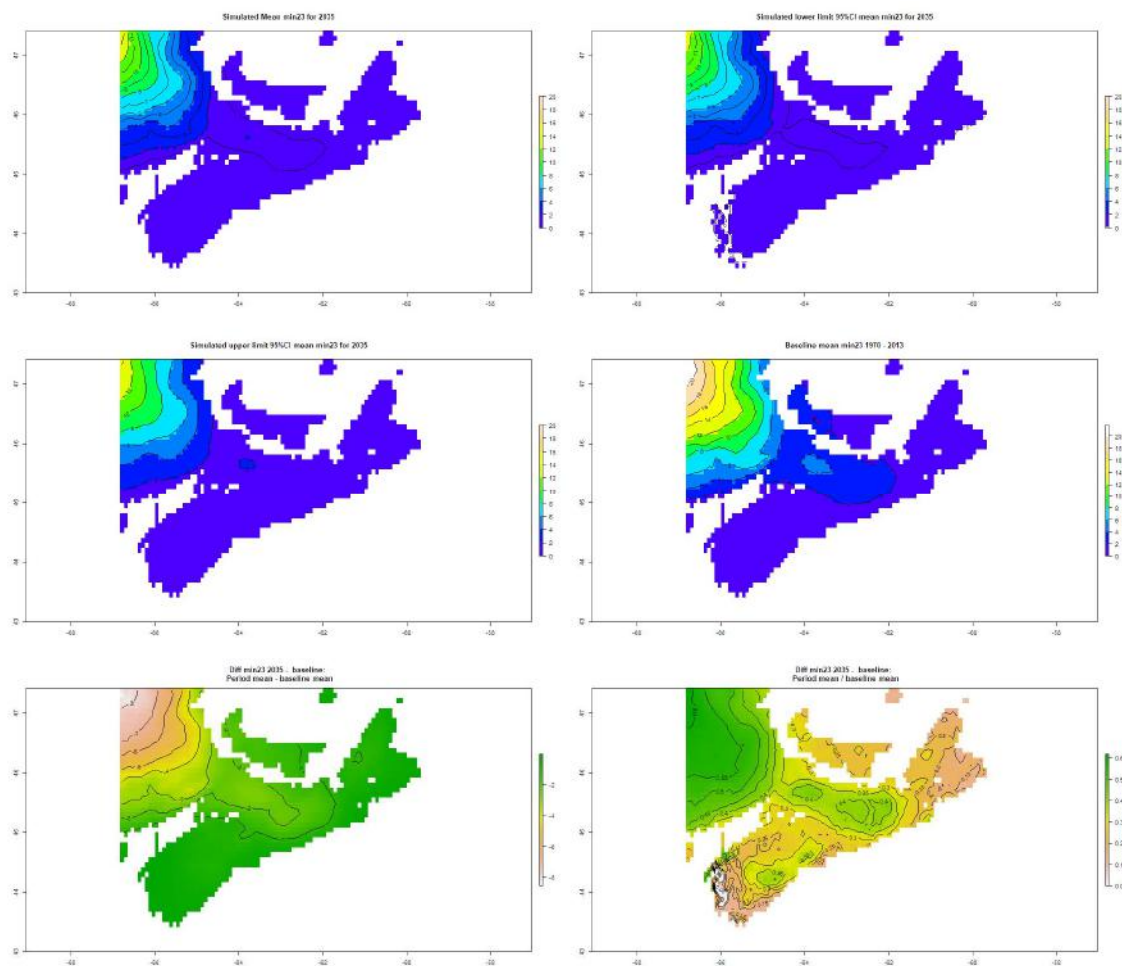


Figure 28. Maps of changes in the number of days less than  $-23^{\circ}\text{C}$  (DL23) relative to the simulated 1970 to 2013 baseline for the 2035 projection period. Top left: simulated mean DL23; top right, lower limit of the 95% CI for the mean; centre left, upper limit to the 95% CI; centre right baseline (modelled) mean DL23 for 1970 to 2013; bottom left, baseline mean minus simulated mean; bottom right, baseline mean / simulated mean.

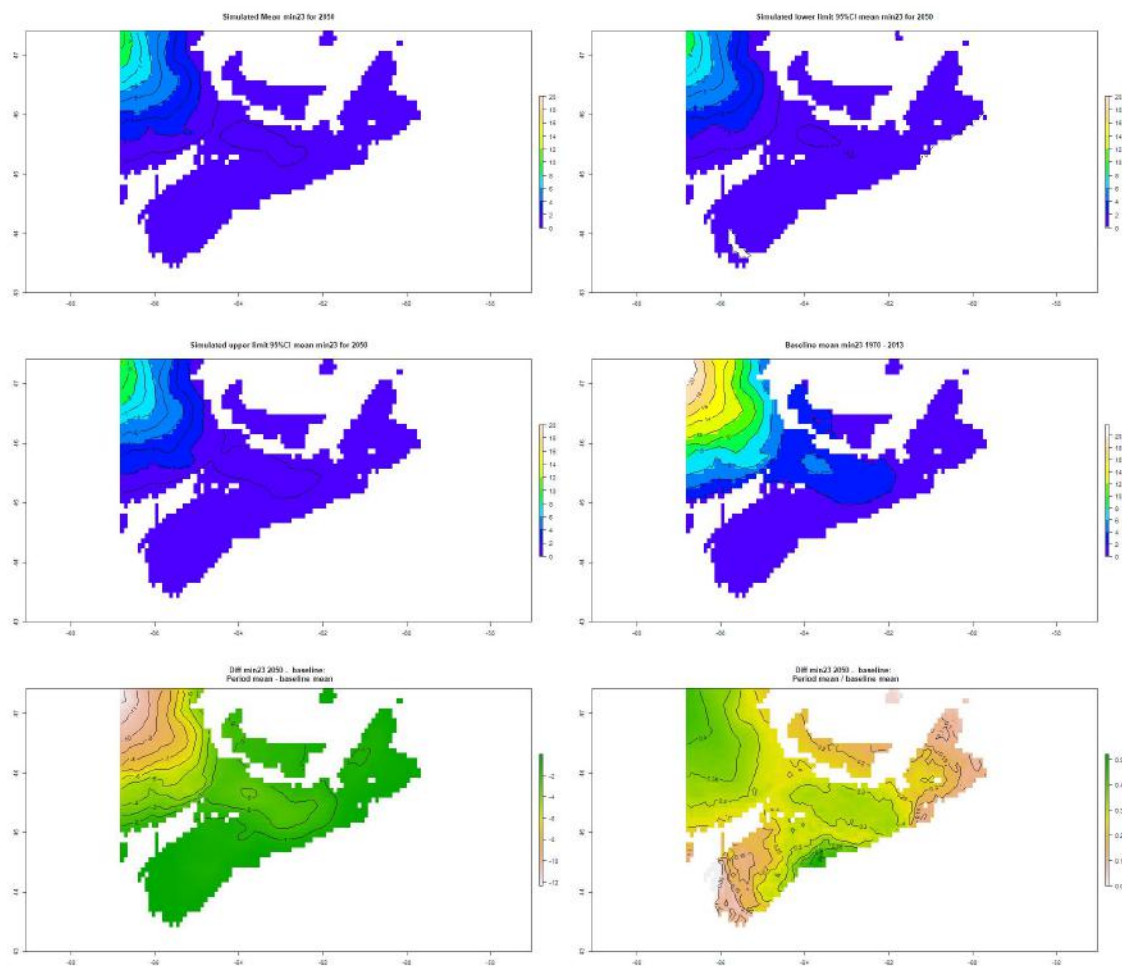


Figure 29. Maps of changes in the number of days less than  $-23^{\circ}\text{C}$  (DL23) relative to the simulated 1970 to 2013 baseline for the 2050 projection period. Top left: simulated mean DL23; top right, lower limit of the 95% CI for the mean; centre left, upper limit to the 95% CI; centre right baseline (modelled) mean DL23 for 1970 to 2013; bottom left, baseline mean minus simulated mean; bottom right, baseline mean / simulated mean.

## Summary

Daily climate station data were provided for 220 locations across Nova Scotia, with varying periods of record for each station. Hourly data were provided for all 9 stations for which hourly data were available.

Climate projection data focused on providing variables required for the grape suitability and grape production models and analyses. Methodologically the data reflect uncertainty in projections due to GCM and downscaling algorithm as well as emissions scenarios. The number of simulation years used for each projection period, and hence results set was 396.

Looking towards 2050 Nova Scotia is likely to experience longer growing seasons with fewer frost days, fewer days of extreme cold and a greater number of very hot days. Accumulated GDD are likely to increase by between 30 and 36% by the 2050 projection period.

The NRCan baseline, 2035 and 2050 projections (GDD, FFD, days < -19°C) data were all used in the grape suitability modelling as planned and the same maps have been used in the GIS data viewer. The projections data have not been used in the grape modelling as the yield data that was available did not enable climate based grape yield or quality estimations. Some of the projection data have been used for the disease modelling.

All of the data that was downloaded and the derived variables have been provided to NSFA. Apps developed using RStudio's Shiny platform have been developed for most of the derived variables will be placed on a NSFA web site for broader public or research access.



## References cited

- Bürger, G., Murdock, T. Q., Werner, A. T., Sobie, S. R., & Cannon, A. J. (2012). Downscaling Extremes—An Intercomparison of Multiple Statistical Methods for Present Climate. *Journal of Climate*, 25(12), 4366-4388. doi:10.1175/jcli-d-11-00408.1
- Bürger, G., Sobie, S. R., Cannon, A. J., Werner, A. T., & Murdock, T. Q. (2013). Downscaling Extremes: An Intercomparison of Multiple Methods for Future Climate. *Journal of Climate*, 26(10), 3429-3449. doi:10.1175/jcli-d-12-00249.1
- Burkner, P.-C. (2017). {brms}: An {R} Package for Bayesian Multilevel Models using Stan.
- Carpenter, B., Gelman, A., Hoffman, M. D., Lee, D., Goodrich, B., Betancourt, M., . . . Riddell, A. (2017). Stan: A probabilistic programming language. *Journal of Statistical Software*, 76(1). doi:10.18637/jss.v076.i01
- Chang, W., Cheng, J., Allaire, J., Xie, Y., & McPherson, J. (2017). shiny: Web Application Framework for R (Version R package version 1.0.5.). Retrieved from <https://CRAN.R-project.org/package=shiny>
- Delignette-Muller, M. L., & Dutang, C. (2015). fitdistrplus: An R Package for Fitting Distributions. *Journal of Statistical Software*, 64(4), 1-34.
- García de Cortázar-Atauri, I., Brisson, N., & Gaudillere, J. P. (2009). Performance of several models for predicting budburst date of grapevine (*Vitis vinifera* L.). *International Journal of Biometeorology*, 53(4), 317-326. doi:10.1007/s00484-009-0217-4
- Hijmans, R. J. (2017). raster: Geographic Data Analysis and Modeling (Version R package version 2.6-7).
- McKenney, D. W., Pedlar, J. H., Papadopol, P., & Hutchinson, M. F. (2006). The development of 1901–2000 historical monthly climate models for Canada and the United States. *Agricultural and Forest Meteorology*, 138(1–4), 69-81. doi:<https://doi.org/10.1016/j.agrformet.2006.03.012>
- Pacific Climate Impacts Consortium. (2014). *Statistically Downscaled Climate Scenarios*. Retrieved from: [http://tools.pacificclimate.org/dataportal/data/downscaled\\_gcms/](http://tools.pacificclimate.org/dataportal/data/downscaled_gcms/)
- Parker, A., Garcia De Cortazar-Atauri, I., Chuine, I., Barbeau, G., Bois, B., Boursiquot, J.-M., . . . Van Leeuwen, C. (2013). Classification of varieties for their timing of flowering and veraison using a modelling approach: A case study for the grapevine species *Vitis vinifera* L. *Agricultural and Forest Meteorology*, 180, 249-264. doi:10.1016/j.agrformet.2013.06.005
- Parker, A. K., De Cortázar-Atauri, I. G., Van Leeuwen, C., & Chuine, I. (2011). General phenological model to characterise the timing of flowering and veraison of *Vitis vinifera* L. *Australian Journal of Grape and Wine Research*, 17(2), 206-216. doi:10.1111/j.1755-0238.2011.00140.x
- Pedlar, J. H., McKenney, D. W., Lawrence, K., Papadopol, P., Hutchinson, M. F., & Price, D. (2015). A Comparison of Two Approaches for Generating Spatial Models of Growing-Season Variables for Canada. *Journal of Applied Meteorology and Climatology*, 54(2), 506-518. doi:10.1175/JAMC-D-14-0045.1
- R Core Team. (2017). R: A Language and Environment for Statistical Computing. Vienna, Austria. Retrieved from <http://www.R-project.org/>
- Scutari, M. (2010). Learning Bayesian Networks with the bnlearn R Package. *Journal of Statistical Software*, 35(3), 1-22.
- Werner, A. T., & Cannon, A. J. (2015). Hydrologic extremes – an intercomparison of multiple gridded statistical downscaling methods. *Hydrology and Earth System Sciences Discussions*, 12, 6179-6239. doi:10.5194/hessd-12-6179-2015
- Winkler, A. J., Cook, J. A., Kliewer, W. M., & Lider, L. A. (1974). *General Viticulture*. Los Angeles: University of California Press.
- Wood, A. W., Leung, L. R., Sridhar, V., & Lettenmaier, D. P. (2004). Hydrologic Implications of Dynamical and Statistical Approaches to Downscaling Climate Model Outputs. *Climatic Change*, 62(1), 189-216. doi:10.1023/B:CLIM.0000013685.99609.9e

## Appendix 1: Climate station data – stations names, ID's and time periods of data downloaded.

Name	Station ID	Latitude	longitude	Elevation	First Year	Last Year	Length	Most recent
BADDECK	6297	46.1	-60.75	7.6	1875	2000	125	2000
NAPPAN CDA	6414	45.77	-64.25	19.8	1890	2005	115	2005
PORT HASTINGS	6441	45.63	-61.4	23.1	1874	1989	115	1989
PARRSBORO	6428	45.4	-64.33	24.3	1897	2002	105	2002
COLLEGEVILLE	6329	45.48	-62.02	76.2	1916	2014	98	2014
ST MARGARET'S BAY	6456	44.7	-63.9	17.4	1922	2017	95	2017
ANNAPOLIS ROYAL	6289	44.75	-65.52	7.7	1914	2007	93	2007
BEAVERBANK	6301	44.9	-63.72	182.9	1871	1964	93	1964
DIGBY	6338	44.62	-65.75	12.2	1872	1965	93	1965
UPPER STEWIAKKE	6495	45.22	-63	22.9	1915	2005	90	2005
MAHONE BAY	6396	44.47	-64.38	25.9	1872	1960	88	1960
MOUNT UNIACKE	6413	44.9	-63.83	158.5	1919	2003	84	2003
SPRINGFIELD	6473	44.67	-64.85	167.3	1919	2003	84	2003
KENTVILLE CDA	6375	45.07	-64.48	48.8	1913	1996	83	1996
WOLFVILLE	6513	45.1	-64.37	41.1	1870	1949	79	1949
WHITEHEAD	6506	45.22	-61.18	13.7	1883	1960	77	1960
WINDSOR KINGS COLLEGE	6511	44.98	-64.1	27.4	1871	1948	77	1948
GREENWOOD A	6354	44.98	-64.92	28	1942	2017	75	2017
SALMON HOLE	6458	44.93	-64.03	83.8	1938	2013	75	2013
SHEARWATER A	6465	44.63	-63.5	44	1944	2017	73	2017
SYDNEY A	6486	46.17	-60.05	61.9	1941	2014	73	2014
LIVERPOOL BIG FALLS	6383	44.13	-64.93	49.6	1940	2012	72	2012
YARMOUTH A	6516	43.83	-66.09	43	1940	2012	72	2012
SYDNEY	6485	46.15	-60.2	14.6	1870	1941	71	1941
YARMOUTH	6515	43.83	-66.03	30.8	1870	1941	71	1941
HALIFAX CITADEL	6357	44.65	-63.58	70.1	1933	2002	69	2002
ANTIGONISH	6290	45.63	-61.97	9.1	1880	1947	67	1947
STILLWATER	6481	45.18	-62	17.1	1915	1979	64	1979
HALIFAX	6355	44.65	-63.6	29.6	1871	1933	62	1933
TRAFALGAR	6489	45.28	-62.67	152.4	1919	1981	62	1981
HALIFAX STANFIELD INT'L A	6358	44.88	-63.5	145.4	1953	2012	59	2012
WESTERN HEAD	6501	43.99	-64.66	10.06	1959	2017	58	2017
TUSKET	6493	43.88	-65.98	9.1	1950	2007	57	2007
TRURO NSAC	6492	45.37	-63.3	23.5	1910	1966	56	1966
DEMING	6336	45.22	-61.18	15.8	1956	2011	55	2011
BEAR RIVER	6300	44.57	-65.63	7.6	1952	2006	54	2006
AVON	6294	44.88	-64.22	23.7	1949	2001	52	2001
BRIDGEWATER	6308	44.4	-64.55	27.4	1961	2013	52	2013
MIDDLE MUSQUODOBOIT	6409	45.07	-63.1	47.8	1961	2013	52	2013



INGONISH BEACH	6368	46.65	-60.4	7.9	1950	2000	50	2000
MALAY FALLS	6399	44.98	-62.48	39.6	1950	2000	50	2000
METEGHAN RIVER	6406	44.27	-66.13	15.2	1937	1986	49	1986
PUGWASH	6447	45.84	-63.66	4.6	1965	2014	49	2014
BRIER ISLAND	10859	44.29	-66.35	15.8	1969	2017	48	2017
LIVERPOOL MILTON	6384	44.08	-64.77	28.5	1966	2013	47	2013
PARADISE	6427	44.83	-65.23	45.7	1950	1997	47	1997
ECUM SECUM	6344	44.98	-62.18	15.3	1940	1986	46	1986
FIVE MILE LAKE	6348	44.95	-64	45.7	1933	1978	45	1978
ROSEWAY	6452	43.78	-65.35	15.2	1950	1995	45	1995
DICKIE BROOK	6337	45.35	-61.5	2.8	1950	1994	44	1994
PORT HOOD	6443	45.98	-61.53	27.4	1950	1993	43	1993
TRURO	6490	45.35	-63.3	12.2	1872	1915	43	1915
WESTPHAL	6503	44.68	-63.52	67.7	1955	1998	43	1998
CHETICAMP	6322	46.65	-60.95	11	1956	1998	42	1998
TRURO	6491	45.37	-63.27	39.9	1960	2002	42	2002
CLIFTON	6326	45.35	-63.42	15.2	1948	1989	41	1989
KEMPTVILLE	6373	44.08	-65.77	76.2	1950	1991	41	1991
LOUISBOURG	6388	45.9	-60	45.7	1972	2013	41	2013
PLEASANT BAY	6434	46.82	-60.77	28.9	1955	1996	41	1996
GRAND ANSE WHITE ROCK	6507	45.05	-64.38	38.1	1977	2017	40	2017
SUMMERVILLE	6484	45.12	-64.18	38.1	1965	2004	39	2004
CAPE SABLE	6315	43.38	-65.62	3	1948	1986	38	1986
POCKWOCK LAKE	6435	44.77	-63.83	164.6	1979	2017	38	2017
FRIZZLETON	6350	46.37	-60.97		1916	1953	37	1953
STILLWATER	6482	45.14	-61.98	14	1967	2004	37	2004
SHERBROOKE WATERVILLE	6497	45.05	-64.65	30.6	1980	2017	37	2017
CAMBRIDGE CHARLESVILLE	6318	43.58	-65.78	2.7	1978	2014	36	2014
HARMONY	6361	44.42	-65.05	106.7	1950	1986	36	1986
PICTOU	6430	45.7	-62.68	24.4	1870	1906	36	1906
WRECK COVE BROOK	6514	46.53	-60.45	76.2	1976	2012	36	2012
CLARENCE	6324	44.92	-65.17	51.5	1958	1993	35	1993
HALIFAX	6356	44.65	-63.57	31.7	1939	1974	35	1974
SHEFFIELD MILLS	6467	45.13	-64.5	30.2	1958	1993	35	1993
WEYMOUTH FALLS	6505	44.4	-65.95	10.7	1965	2000	35	2000
LYONS BROOK	6393	45.66	-62.8	28.9	1984	2017	33	2017
PORT MORIEN	6444	46.13	-59.87		1873	1906	33	1906
CHAIN LAKE	6317	44.63	-63.63	59.4	1945	1977	32	1977
MIDDLETON	6410	44.95	-65.07	21.3	1914	1946	32	1946
NORTHEAST MARGAREE	6423	46.35	-61	31.1	1955	1987	32	1987
SPRUCE HILL LAKE	6476	44.58	-63.65	107.6	1945	1977	32	1977
WESTPORT	6504	44.25	-66.37	18.2	1961	1993	32	1993
COPPER LAKE	6330	45.38	-61.97	96.9	1945	1974	29	1974
KEJIMKUJIK PARK	6372	44.43	-65.2	126.8	1966	1994	28	1994

MABOU	6394	46.07	-61.38	32	1986	2014	28	2014
MARGAREE FORKS	6401	46.33	-61.1	22.9	1976	2004	28	2004
ST PAUL ISLAND	6457	47.2	-60.15	31.7	1928	1956	28	1956
LAKE ROSSIGNOL	6377	44.22	-65.23	85.3	1941	1967	26	1967
LIVERPOOL	6382	44.07	-64.67	15.2	1913	1939	26	1939
LOWER MEAGHERS GRANT	6390	44.92	-63.23	41.1	1967	1993	26	1993
NOEL	6419	45.28	-63.73	45.7	1934	1960	26	1960
OXFORD	6426	45.73	-63.87	12.8	1953	1979	26	1979
SANDY COVE NRC	6461	44.47	-63.57	10.1	1975	2001	26	2001
WINDSOR FALMOUTH	6510	44.98	-64.17	14.6	1962	1988	26	1988
WINDSOR MARTOCK	6512	44.93	-64.17	38.1	1979	2005	26	2005
RUTH FALLS	6453	44.93	-62.5	7.6	1961	1986	25	1986
BEAVER ISLAND (AUT)	10078	44.82	-62.33	16	1992	2017	25	2017
GREAT VILLAGE	6353	45.42	-63.62	22	1980	2004	24	2004
INDIAN BROOK	6367	46.37	-60.53	13.2	1965	1989	24	1989
STELLARTON LOURDES	6479	45.57	-62.65	10.7	1952	1976	24	1976
KEJIMKUJIK 1	6923	44.4	-65.2	125	1993	2017	24	2017
TATAMAGOUCHE	6927	45.68	-63.23	18	1993	2017	24	2017
HART ISLAND (AUT)	7173	45.35	-60.98	8.2	1993	2017	24	2017
CARIBOU POINT (AUT)	8990	45.77	-62.68	2.4	1993	2017	24	2017
ST PAUL ISLAND (AUT)	9033	47.23	-60.14	27	1993	2017	24	2017
AYLESFORD	6295	45.03	-64.87	39.9	1961	1984	23	1984
MIDDLEBORO	6407	45.77	-63.57	30.5	1981	2004	23	2004
POINT ACONI	6437	46.32	-60.33	11.7	1990	2013	23	2013
NORTHEAST MARGAREE (AUT)	10661	46.37	-60.98	54	1994	2017	23	2017
GRAND ETANG	10792	46.55	-61.05	12.8	1994	2017	23	2017
SHEARWATER JETTY	10945	44.63	-63.52	5.5	1994	2017	23	2017
BACCARO	6296	43.47	-65.47	3	1957	1979	22	1979
BARRIE BROOK	6298	45.65	-61.43	10.7	1950	1972	22	1972
JACKSON	6370	45.58	-63.83	91.4	1982	2004	22	2004
RIVER DENYS	6449	45.8	-61.22	27.4	1966	1988	22	1988
FARMINGTON	6347	44.63	-64.67	151.5	1982	2003	21	2003
SAULNIERVILLE	6462	44.27	-66.12	45.7	1916	1937	21	1937
SOUTH ALTON	6470	45.07	-64.53		1912	1933	21	1933
KENTVILLE CDA CS	27141	45.07	-64.48	48.7	1996	2017	21	2017
DIGBY PRIM POINT	6341	44.68	-65.78	21.3	1965	1985	20	1985
MILL VILLAGE	6412	44.18	-64.67	15.2	1973	1993	20	1993
RAWDON	6448	45.05	-63.78	182.9	1956	1976	20	1976
BIRCHTOWN	6304	45.45	-61.48	68.6	1958	1977	19	1977
CLEMENTSVALE	6325	44.62	-65.57	106.7	1961	1980	19	1980
DEBERT	6334	45.42	-63.42	38.1	1982	2001	19	2001

LIVERPOOL	6381	44.05	-64.72	5.5	1940	1959	19	1959
NORTHEAST	6422	46.33	-60.97	83.8	1955	1974	19	1974
MARGAREE PORT	6442	45.65	-61.38	114.9	1985	2004	19	2004
HAWKESBURY A STELLARTON	6478	45.57	-62.65	7.6	1940	1959	19	1959
BERWICK	7105	45.08	-64.73	39.6	1994	2013	19	2013
NORTH	27592	46.82	-60.67	439.4	1998	2017	19	2017
MOUNTAIN CS CHETICAMP CS	27600	46.65	-60.95	43.9	1998	2017	19	2017
RIVER HEBERT	6450	45.6	-64.35	24.4	1962	1980	18	1980
MCNABS ISLAND (AUT)	7169	44.6	-63.53	15.4	1999	2017	18	2017
LAKE MAJOR	27742	44.72	-63.48	62.5	1999	2017	18	2017
MALAY FALLS	30668	44.98	-62.48	39.6	1999	2017	18	2017
NEW GRAFTON	6418	44.42	-65.18		1950	1967	17	1967
TIMBERLEA	6488	44.67	-63.75	83.8	1946	1963	17	1963
INGONISH BEACH RCS	30326	46.66	-60.41	10	2000	2017	17	2017
HOPEWELL	6365	45.5	-62.72	152.4	1968	1984	16	1984
LOWER L'ARDOISE	6389	45.6	-60.75	15.2	1974	1990	16	1990
SHELBURNE	6468	43.72	-65.25	29.9	1972	1988	16	1988
DEBERT A	6335	45.42	-63.45	44.2	1945	1960	15	1960
DIGBY CKDY	6340	44.62	-65.77	60.7	1970	1985	15	1985
LOCH LOMOND	6385	45.73	-60.62	30.5	1958	1973	15	1973
MARGAREE FORKS	6400	46.37	-61.08	15.2	1960	1975	15	1975
SPRINGHILL	6475	45.62	-64.07	170.1	1982	1997	15	1997
BACCARO POINT	10914	43.45	-65.47	12.7	1994	2009	15	2009
LUNENBURG	31829	44.36	-64.3	3.8	2002	2017	15	2017
EDDY POINT	6345	45.52	-61.25	66.1	1971	1985	14	1985
SHEARWATER AUTO	27223	44.64	-63.51	53	1996	2010	14	2010
SOUTH SIDE HARBOUR	27282	45.62	-61.9	30	1997	2011	14	2011
BRIDGETOWN	27930	44.83	-65.3	8	1998	2012	14	2012
TRACADIE	41575	45.61	-61.68	66.67	2003	2017	14	2017
NAPPAN AUTO	42083	45.76	-64.24	19.8	2003	2017	14	2017
DEBERT	42243	45.42	-63.47	37.5	2003	2017	14	2017
INVERNESS (AUT)	6369	46.23	-61.3	38.9	1973	1986	13	1986
MARGAREE HARBOUR	6402	46.43	-61.1	5.5	1958	1971	13	1971
AVONDALE	6921	45.02	-64.12	42.1	1993	2006	13	2006
AMHERST (AUT)	7103	45.85	-64.27	23	1992	2005	13	2005
TRURO (AUT)	7162	45.37	-63.27	39.9	1992	2005	13	2005
BEDFORD RANGE	43123	44.75	-63.66	9.6	2004	2017	13	2017
HALIFAX	43124	44.59	-63.55	52	2004	2017	13	2017
KOOTENAY PARRSBORO	43183	45.41	-64.35	30.89	2004	2017	13	2017
HALIFAX WINDSOR PARK	43403	44.66	-63.61	51	2004	2017	13	2017
OSBORNE HEAD DND	43404	44.61	-63.42	30	2004	2017	13	2017

HALIFAX DOCKYARD	43405	44.66	-63.58	3.8	2004	2017	13	2017
BEDFORD BASIN	43406	44.71	-63.63	3.5	2004	2017	13	2017
BEDFORD	6302	44.73	-63.67	30.5	1954	1966	12	1966
FRASER BROOK IHD	6349	45.33	-63.17	121.9	1965	1977	12	1977
SHEET HARBOUR	6466	44.92	-62.48	9.1	1950	1962	12	1962
TATAMAGOUCHE	6487	45.75	-63.37	7.6	1966	1978	12	1978
SOUTH MOUNTAIN	26969	45.02	-64.68	134.7	1994	2006	12	2006
UPPER STEWIAKKE RCS	44363	45.23	-63.06	23.5	2005	2017	12	2017
MALAGASH POINT	6398	45.78	-63.28	7.6	1989	2000	11	2000
SHARPE BROOK IHD	6464	45.02	-64.63	137.2	1967	1978	11	1978
SPRINGHILL	6474	45.62	-64.08	182.9	1918	1929	11	1929
SABLE ISLAND	26864	43.93	-60	4	1995	2006	11	2006
SYDNEY CS	44503	46.16	-60.04	62.5	2006	2017	11	2017
APRIL BROOK IHD	6292	46.23	-61.13	61	1966	1976	10	1976
CHETICAMP	6321	46.63	-61.05	335.3	1935	1945	10	1945
INVERNESS	6922	46.2	-61.3	35.1	1991	2001	10	2001
BADDECK BELL	30386	46.1	-60.75	16.6	2000	2010	10	2010
BACCARO PT	46007	43.45	-65.47	4.6	2007	2017	10	2017
BRAESHORE	6307	45.7	-62.65	7.6	1975	1984	9	1984
DAYTON	6333	43.87	-66.1	8.9	1988	1997	9	1997
POINT TUPPER	6438	45.58	-61.33	29	1970	1979	9	1979
WENTWORTH	6498	45.7	-63.55	45.7	1957	1966	9	1966
SHEARWATER RCS	47187	44.63	-63.51	24	2008	2017	9	2017
BIG INTERVALE	6303	46.83	-60.62	39.6	1984	1992	8	1992
CANSO	6312	45.32	-60.97	25.9	1963	1971	8	1971
DIGBY AIRPORT	6339	44.55	-65.78	152.1	1989	1997	8	1997
GARLAND	6351	45.12	-64.78	205.7	1964	1972	8	1972
HUBBARDS	6366	44.63	-64.08	30.5	1972	1980	8	1980
LISCOMB GAME SANCTUARY	6380	45.05	-62.5	61	1962	1970	8	1970
LORNE STATION	6387	45.43	-62.72	118.9	1984	1992	8	1992
LOWER SACKVILLE	6391	44.77	-63.67	48.8	1964	1972	8	1972
NEW GERMANY	6416	44.55	-64.7	78.6	1952	1960	8	1960
CAPE GEORGE	10936	45.87	-61.9	120	1994	2002	8	2002
CORNWALL	6331	44.53	-64.57		1950	1957	7	1957
EAST JORDAN	6342	43.73	-65.2	15.2	1973	1980	7	1980
GLENORA FALLS	6352	46.12	-61.37	76.2	1954	1961	7	1961
RIVER JOHN	6451	45.75	-63.12	13.1	1979	1986	7	1986
MILFORD STATION	6924	45.03	-63.4	31.5	1993	2000	7	2000
PORT HAWKESBURY	48668	45.66	-61.37	114.9	2010	2017	7	2017
CAMDEN IHD	6310	45.32	-63.2	182.9	1973	1979	6	1979
YARMOUTH CDA EPF	6517	43.93	-66.12	38.1	1956	1962	6	1962
TRENTON MUNICIPAL A	27868	45.61	-62.62	97.23	1999	2005	6	2005

ESKASONI FIRST NATION AUTOMATIC WEATHER STATION	49748	45.92	-60.65	28	2011	2017	6	2017
ABERCROMBIE POINT	6288	45.65	-62.72	10.7	1973	1978	5	1978
CAMBRIDGE STATION	6309	45.07	-64.62	30.5	1973	1978	5	1978
CLYDESDALE	6327	45.63	-62.03	56.7	1990	1995	5	1995
EAST RIVER ST MARY'S	6343	45.38	-62.17	52.4	1975	1980	5	1980
HOLLOW BRIDGE	6364	45	-64.38	127.7	1950	1955	5	1955
LOCH LOMOND	6386	45.73	-60.6	45.7	1973	1978	5	1978
MIDDLE CLYDE RIVER	6408	43.85	-65.52	53.3	1990	1995	5	1995
NEW GLASGOW TRENTON	6417	45.62	-62.62	93.3	1945	1950	5	1950
SEAFOAM	6463	45.78	-62.97	16.8	1984	1989	5	1989
URBANIA	6496	45.22	-63.43	61.9	1986	1991	5	1991
YARMOUTH A	50133	43.83	-66.09	42.9	2012	2017	5	2017
YARMOUTH RCS	50408	43.83	-66.09	36	2012	2017	5	2017
HALIFAX INTL A	50620	44.88	-63.51	145.4	2012	2017	5	2017

